

2,2'-Ethylenebis(1,3-dithiane) as polydentate μ_2 -, μ_4 - and μ_5 -
assembling ligand for the construction of sulphur-rich Cu(I),
Hg(II) and heterometallic Cu(I)/Hg(II) coordination polymers
featuring uncommon network architectures

Lydie Viau,^{*[a]} Michael Knorr,^{*[a]} Lena Knauer,^[b] Lukas Brieger,^[b] and Carsten
Strohmann^{*[b]}

Table of contents

Figure S1. View down the <i>b</i> axis of three layers of the 2D network of $\{[\text{Cu}(\mu_2\text{-I})_2\text{Cu}\}(\mu_2\text{-L1})_2\}_n$ CP1	3
Figure S2. View down the <i>c</i> axis of two layers of the 2D network of $\{[\text{Cu}(\mu_2\text{-I})_2\text{Cu}\}(\mu_4\text{-L1})\}_n$ CP2	4
Figure S3. View down the <i>a</i> axis of the <i>bc</i> plane of CP3	4
Figure S4. View down the <i>c</i> axis on the <i>ab</i> plane showing two layers of the 2D network of $\{[\text{Cu}(\mu_2\text{-Br})_2(\mu_2\text{-L1})(\mu_4\text{-L1})_{0.5}\}_n$ (CP4).	5
Figure S5. View down the <i>c</i> axis on the <i>ab</i> plane showing two layers of the 2D network of $\{[\text{Cu}(\mu_2\text{-Br})_2(\mu_4\text{-L1})\}_n$ CP5	6
Figure S6. A view along the <i>b</i> axis of the crystal packing of CP6 . The C—H···Br hydrogen bonds are shown as dashed lines.....	7
Figure S7. View down the <i>c</i> axis on the <i>ab</i> plane showing two layers of the 2D network of $\{[\text{Cu}(\mu_2\text{-Cl})_2\text{Cu}\}(\mu_4\text{-L1})\}_n$ CP7	8
Figure S8. View of the unit cell of CP9 containing two parallel running 1D ribbons.	8
Figure S9. View of the packing of the ribbons of CP10 within the unit cell.....	9
Figure S10. View of the association of parallel running 1D chains of $[(\text{HgBr}_2)(\mu_2\text{-L2})\}_n$ (CP11) through intermolecular H...Br bonding generating a 3D supramolecular network.	9
Figure S11. Parallel arrangement of the ribbons of CP13 in the packing.	10
Figure S12. View of the packing of three layers of the 2D network of $\{[\text{Cu}(\text{MeCN})](\text{HgIBr}_2)(\mu_2\text{-L1})_{1.5}\}_n$ (CP15).	10
Figure S13. Simulated and experimental PXRD patterns of CP1	11
Figure S14. Simulated and experimental PXRD patterns of CP2	11
Figure S15. Simulated and experimental PXRD patterns of CP3	12
Figure S16. PXRD pattern of CP1 before and after heating at 300°C. Arrows and asterisk are assigned to CP3 and $\gamma\text{-CuI}$ respectively.	12
Figure S17. PXRD pattern of CP1 before and after addition of 1 equivalent Cul. Comparison with the PXRD of CP3	13
Figure S18. Simulated and experimental PXRD patterns of CP4	13
Figure S19. Simulated and experimental PXRD patterns of CP5	14
Figure S20. PXRD patterns of CP6 before and after exposure to NEt_3	14
Figure S21. Simulated and experimental PXRD patterns of CP7	15
Figure S22. Simulated and experimental PXRD patterns of CP8	15
Figure S23. Simulated and experimental PXRD patterns of CP9	16
Figure S24. Simulated and experimental PXRD patterns of CP12	16
Figure S25. Simulated and experimental PXRD patterns of CP13	17

Figure S26. Experimental PXRD patterns of CP13 obtained by addition of 1CuI to CP8 and of 1HgI ₂ to CP1	17
Figure S27. Simulated and experimental PXRD patterns of CP14	18
Figure S28. Simulated and experimental PXRD patterns of CP15	18
Figure S29. ATR-IR spectrum of CP6	19
Figure S30. IR spectra of CP6 before and after exposure to NEt ₃	19
Figure S31. ATR-IR spectrum of CP13	20
Figure S32. ATR-IR spectrum of CP14	20
Figure S33. ATR-IR spectrum of CP15	21
Figure S34. TGA traces and its first derivatives of CP1 under air flow.....	21
Figure S35. TGA traces and its first derivatives of CP2 under air flow.....	22
Figure S36. TGA traces and its first derivatives of CP3 under air flow.....	22
Figure S37. TGA traces and its first derivatives of CP4 under air flow.....	23
Figure S38. TGA traces and its first derivatives of CP5 under air flow.....	23
Figure S39. TGA traces and its first derivatives of CP6 under air flow.....	24
Figure S40. TGA traces and its first derivatives of CP7 under air flow.....	24
Figure S41. Images of CP6 before and after exposure to NEt ₃ vapor.	25
Table S1. Crystal Data, Data Collection and Structure Refinement for L1 and CP1	26
Table S2. Crystal Data, Data Collection and Structure Refinement for CP2 and CP3	27
Table S3. Crystal Data, Data Collection and Structure Refinement for CP4 and CP5	28
Table S4. Crystal Data, Data Collection and Structure Refinement for CP6 at 100K and 200K.	29
Table S5. Crystal Data, Data Collection and Structure Refinement for CP7 and CP8	30
Table S6. Crystal Data, Data Collection and Structure Refinement for CP9 and CP10	31
Table S7. Crystal Data, Data Collection and Structure Refinement for CP11 and CP13	32
Table S8. Crystal Data, Data Collection and Structure Refinement for CP14 and CP15	33
Table S9. Crystal Data, Data Collection and Structure Refinement for D1 and M1	34
Table S10. Hydrogen bond geometry (Å, °) in CP6	35
Table S11. Hydrogen bond geometry (Å, °) in CP11	35

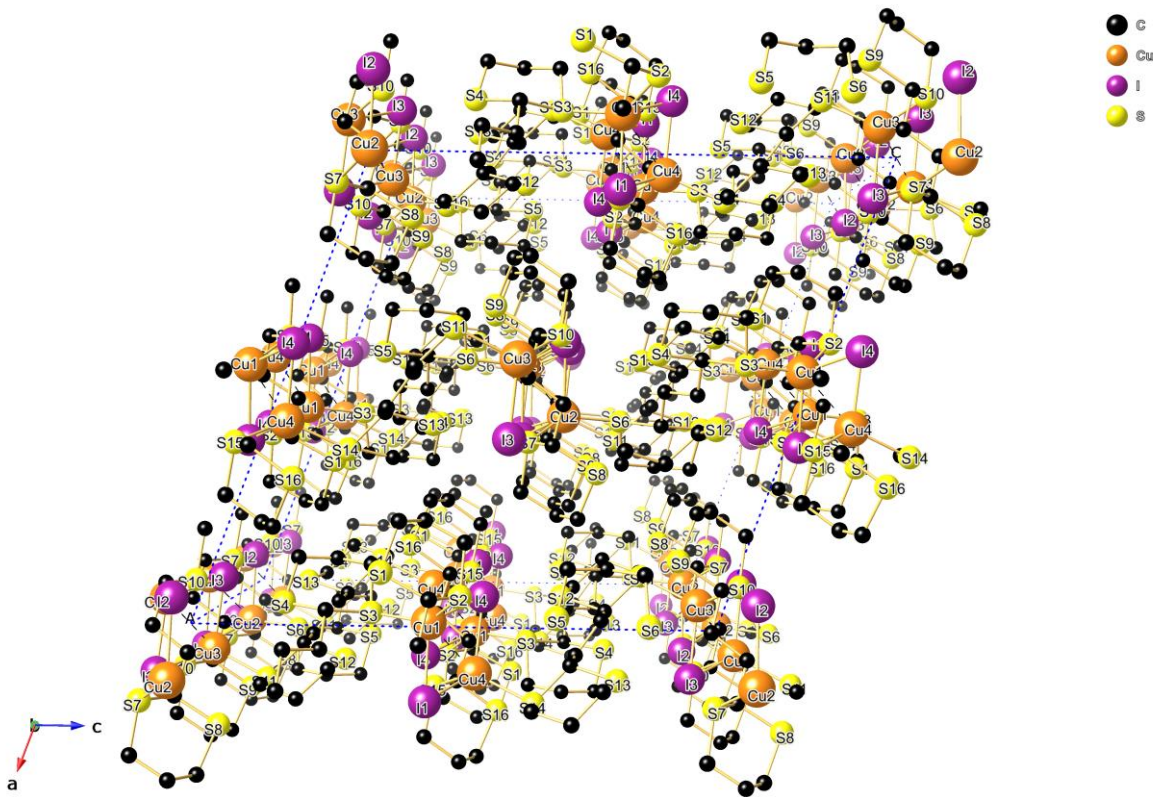


Figure S1. View down the *b* axis of three layers of the 2D network of $[\{\text{Cu}(\mu_2\text{-I})_2\text{Cu}\}(\mu_2\text{-L1})_2]_n$ **CP1**.

Selected angles ($^\circ$) at 100 K: Cu1A-I1A-Cu4¹ 65.144(10), Cu2-I2A-Cu2² 64.360(9), Cu3-I3-Cu3³ 66.954(9), Cu4-I4-Cu1A⁴ 65.427(9), I1A-Cu1A-I4¹ 114.236(11), I1A-Cu1A-Cu4¹ 57.537(7), I4¹-Cu1A-Cu4¹ 56.950(8), S2-Cu1A-I1A 108.639(15), S2-Cu1A-I4¹ 94.816(15), S2-Cu1A-Cu4¹ 116.447(17), S2-Cu1A-S3 136.45(2), S3-Cu1A-I1A 98.417(17), S3-Cu1A-I4¹ 104.548(16), S3-Cu1A-Cu4¹ 106.776(16), I2A-Cu2-I2A² 115.641(9), I2A²-Cu2-Cu2² 57.281(8), I2A-Cu2-Cu2² 58.361(8), S6-Cu2-I2A² 97.718(14), S6-Cu2-I2A 99.428(14), S6-Cu2-Cu2² 106.242(16), S7-Cu2-I2A 96.568(14), S7-Cu2-I2A² 106.490(14), S7-Cu2-Cu2² 112.012(16), S7-Cu2-S6 141.460(19), I3-Cu3-I3³ 113.046(8), I3³-Cu3-Cu3³ 57.325(8), I3-Cu3-Cu3³ 57.325(8), S10-Cu3-I3³ 93.476(13), S10-Cu3-I3 108.460(14), S10-Cu3-Cu3³ 109.864(15), S10-Cu3-S11 121.608(18), S11-Cu3-I3 111.015(14), S11-Cu3-I3³ 108.138(14), S11-Cu3-Cu3³ 127.358(17), I1A⁴-Cu4-Cu1A⁴ 57.318(9), I4-Cu4-I1A⁴ 114.687(10), I4-Cu4-Cu1A⁴ 57.624(8), S14-Cu4-I1A⁴ 103.824(15), S14-Cu4-I4 110.421(14), S14-Cu4-Cu1A⁴ 127.750(17), S15-Cu4-I1A⁴ 95.011(13), S15-Cu4-I4 105.353(13), S15-Cu4-Cu1A⁴ 104.282(14), S15-Cu4-S14 126.926(18). Symmetry transformations used to generate equivalent atoms: ¹+*x*,+*y*,*z*; ²1-*x*, 2-*y*, 1-*z*; ³1-*x*, 1-*y*,1-*z*; ⁴+*x*,+*y*,-1+*z*.

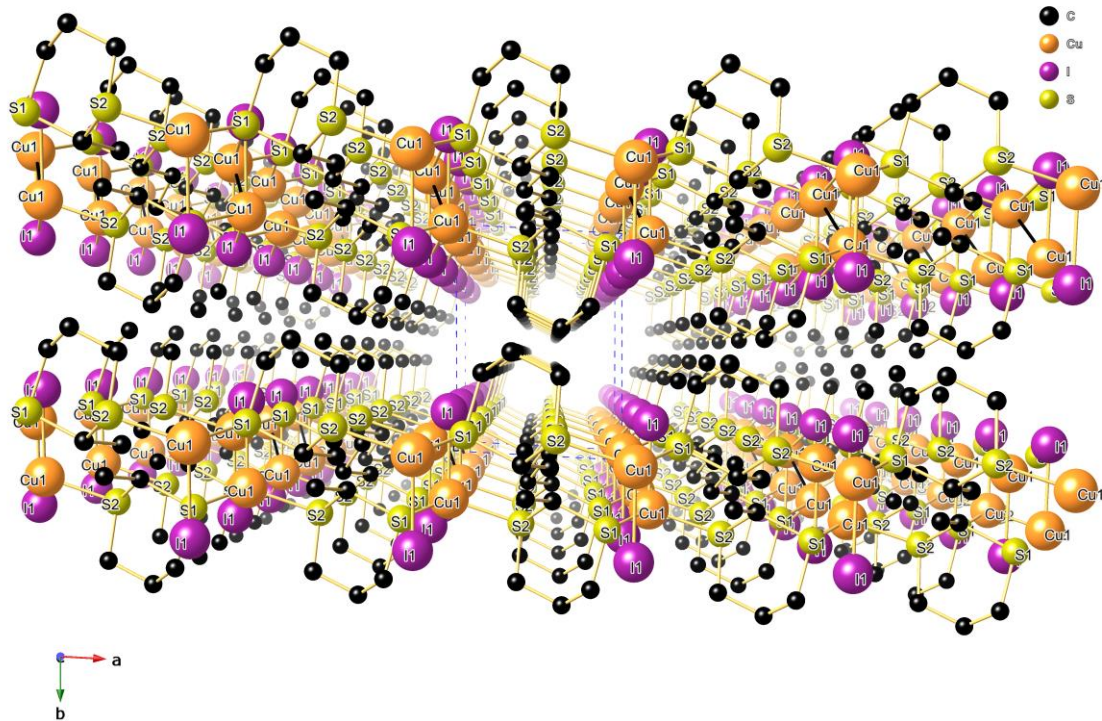


Figure S2. View down the *c* axis of two layers of the 2D network of $\{[\text{Cu}(\mu_2\text{-I})_2\text{Cu}\}(\mu_4\text{-L1})\}_n$ **CP2**.

Selected angles ($^\circ$) at 100 K: S1–Cu–S2 118.02(3), S1–Cu–I 118.40(3), S1–Cu–I# 94.81(3), S2–Cu–I 97.77(3), S2–Cu–I# 107.86(3), I–Cu–I# 121.050(17), Cu–I–Cu# 58.950(17). Symmetry transformations used to generate equivalent atoms: $^1-x, 2-y, 1-y$; $^2-1+x, +y, +z$; $^31-x, 2-y, 2-z$.

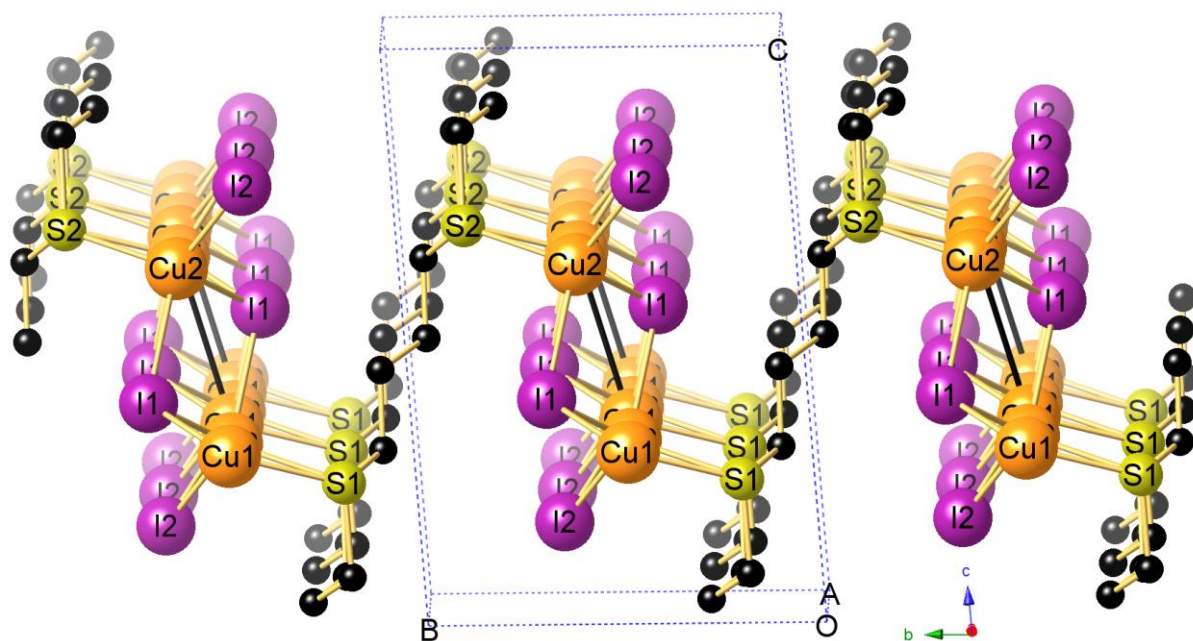


Figure S3. View down the *a* axis of the *bc* plane of **CP3**.

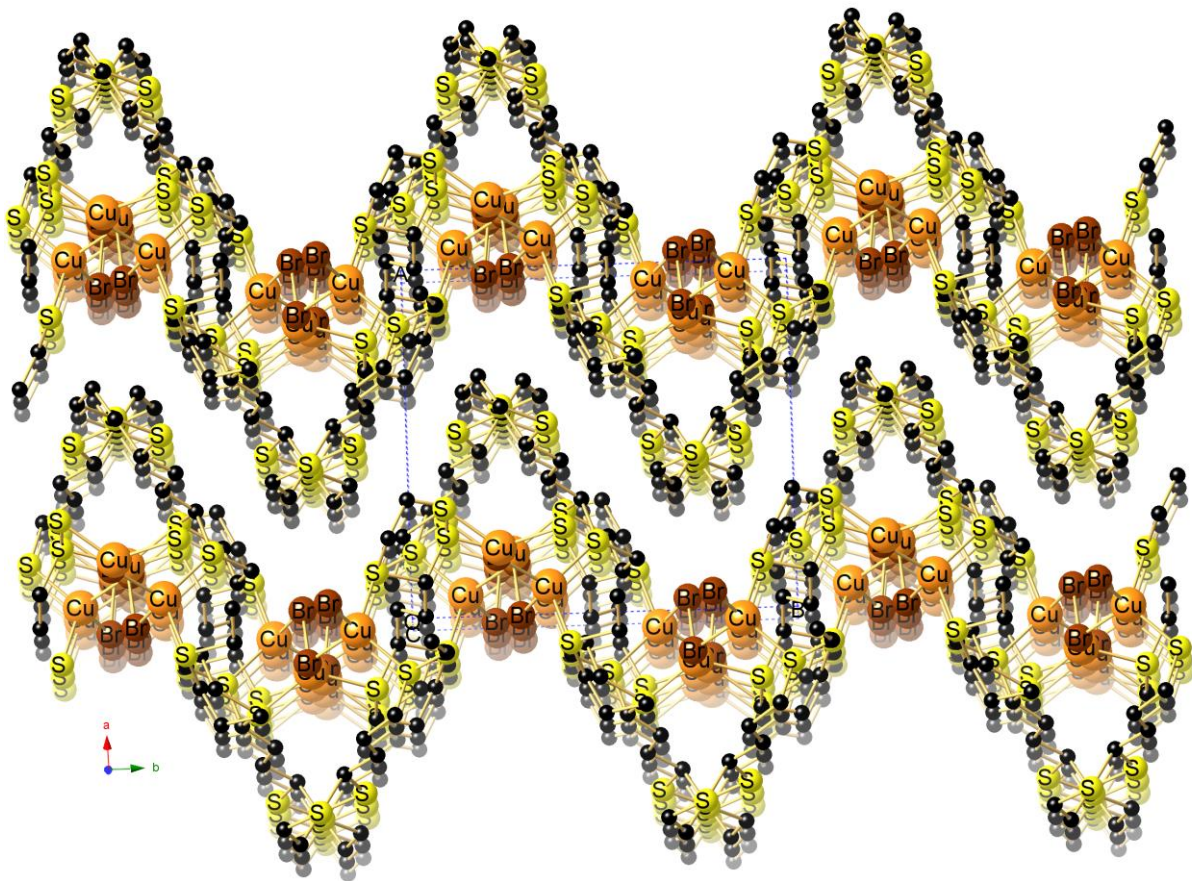


Figure S4. View down the c axis on the ab plane showing two layers of the 2D network of $[\{\text{Cu}(\mu_2\text{-Br})\}_2(\mu_2\text{-L1})(\mu_4\text{-L1})_{0.5}]_n$ (**CP4**).

Selected bond angles [$^\circ$] at 100 K: Cu2–Br1–Cu1 97.945(19), Cu2–Br2–Cu1¹ 127.267(17), Br1–Cu1–Br2² 113.937(19), S1–Cu1–Br1 105.47(2), S1–Cu1–Br2² 100.66(2), S3–Cu1–Br1 112.49(2), S3–Cu1–Br2² 98.30(2), S3–Cu1–S1 125.31(3), Br1–Cu2–Br2 111.701(18), Br1–Cu2–Br2 111.701(18), S2³–Cu2–Br1 101.31(3), S2³–Cu2–Br2 106.02(2), S4–Cu2–Br1 114.21(2), S4–Cu2–Br2 109.49(3), S4–Cu2–S2³ 113.64(3). Symmetry transformations used to generate equivalent atoms: $^1+x, \frac{1}{2}-y, \frac{1}{2}+z; ^21-x, 1-y, 1-z; ^3+x, \frac{1}{2}-y, +z, ^41-x, -\frac{1}{2}+y, \frac{1}{2}-z, ^51-x, \frac{1}{2}+y, \frac{1}{2}-z$.

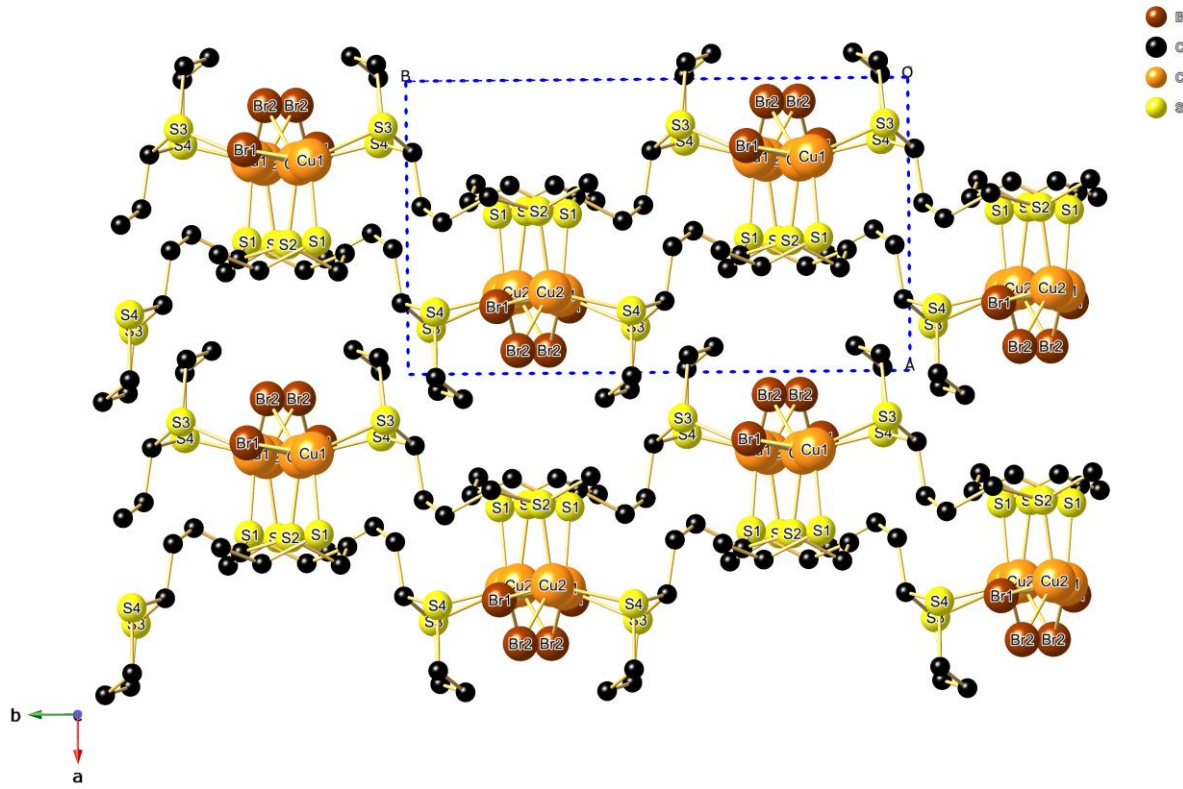


Figure S5. View down the c axis on the ab plane showing two layers of the 2D network of $[\{\text{Cu}(\mu_2\text{-Br})\}_2(\mu_4\text{-L1})]_n \text{CP5}$.

Selected bond angles [$^\circ$] at 100 K: S1–Cu1–S3⁴ 111.34(3), S2–Cu2–S4³ 110.63(3), Cu1–Br1–Cu2¹ 95.446(17), Cu1–Br2–Cu2 100.585(17), Br1–Cu1–Br2 110.070(17), S1–Cu1–Br1 107.80(2), S1–Cu1–Br2 117.62(2), S3⁴–Cu1–Br1 113.18(2), S3⁴–Cu1–Br2 96.68(2), Br2–Cu2–Br1² 103.363(17), S2–Cu2–Br1² 101.45(2), S2–Cu2–Br2 118.97(2), S4³–Cu2–Br1² 122.25(2), S4³–Cu2–Br2 101.16(2) Symmetry transformations used to generate equivalent atoms: $^1x, \frac{1}{2}-y, \frac{1}{2}+z; ^2+x, \frac{1}{2}-y, \frac{1}{2}+z; ^31-x, -1/2+y, 1/2-z; ^41-x, 1-y, 1-z$.

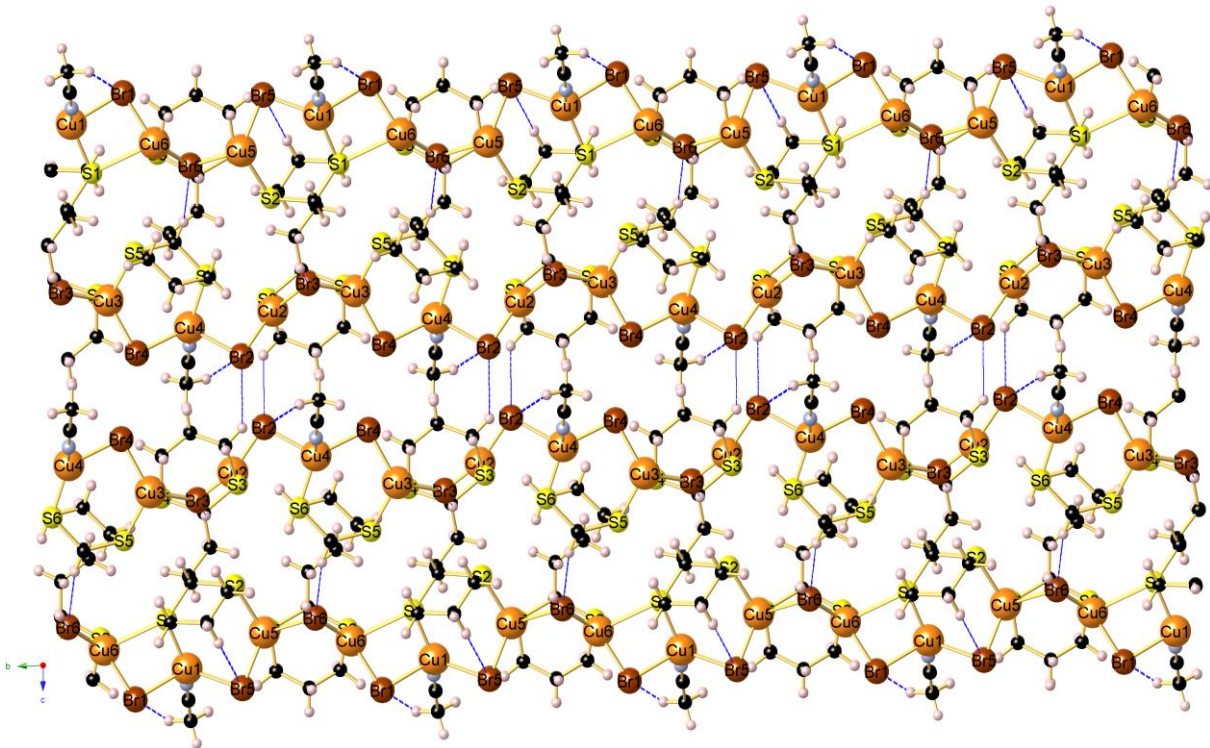


Figure S6. A view along the b axis of the crystal packing of **CP6**. The C—H \cdots Br hydrogen bonds are shown as dashed lines.

Selected bond angles [$^\circ$] at 100 K: Cu6-Br1-Cu1 86.095(11), Cu2-Br2-Cu4¹ 85.690(10), Cu2-Br3-Cu3 86.593(10), Cu3-Br4-Cu4 88.610(10), Cu5-Br5-Cu1² 87.092(10), Cu6-Br6-Cu5 90.168(10), Br5¹-Cu1-Br1 114.647(11), S1-Cu1-Br1 88.147(13), S1-Cu1-Br5¹ 116.754(14), N1-Cu1-Br1 102.761(5), N1-Cu1-Br5¹ 103.15(5), N1-Cu1-S1 129.55(5), Br3-Cu2-Br2 113.534(11), S3-Cu2-Br2 119.320(15), S3-Cu2-Br3 127.119(15), Br4-Cu3-Br3 110.546(11), S4-Cu3-Br3 119.028(143), S4-Cu3-Br4 110.145(14), S4-Cu3-S5 110.445(17), S5-Cu3-Br3 89.848(13), S5-Cu3-Br4 115.767(14), Br4-Cu4-Br2² 110.040(10), S6-Cu4-Br2² 92.521(14), S6-Cu4-Br4 119.944(14), N2-Cu4-Br2² 101.94(5), N2-Cu4-Br4 100.99(5), N2-Cu4-S6 128.49(5), Br5-Cu5-Br6 111.723(10), S2²-Cu5-Br5 118.267(14), S2²-Cu5-Br6 91.616(13), S7-Cu5-Br5 108.229(143), S7-Cu5-Br6 116.736(13), S7-Cu5-S2² 109.898(16), Br1-Cu6-S1 81.800(12), Br6-Cu6-Br1 118.119(12), Br6-Cu6-S1 105.731(14), S8-Cu6-Br1 114.194(15), S8-Cu6-Br6 125.243(15), S8-Cu6-S1 96.326(16), Cu1-S1-Cu6 84.189(15) Symmetry transformations used to generate equivalent atoms: $^1+x, -1+y, +z$; $^2+x, 1+y, +z$.

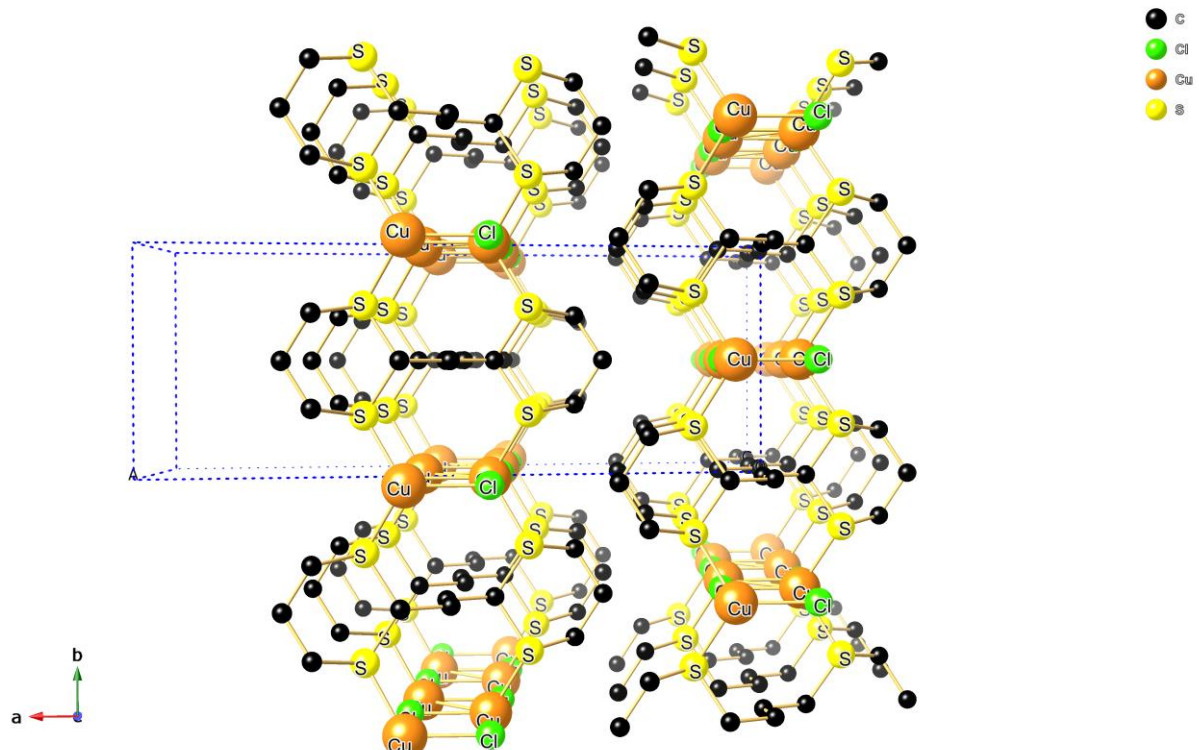


Figure S7. View down the *c* axis on the *ab* plane showing two layers of the 2D network of $[\{\text{Cu}(\mu_2\text{-Cl})_2\text{Cu}\}(\mu_4\text{-L1})]_n \text{CP7}$.

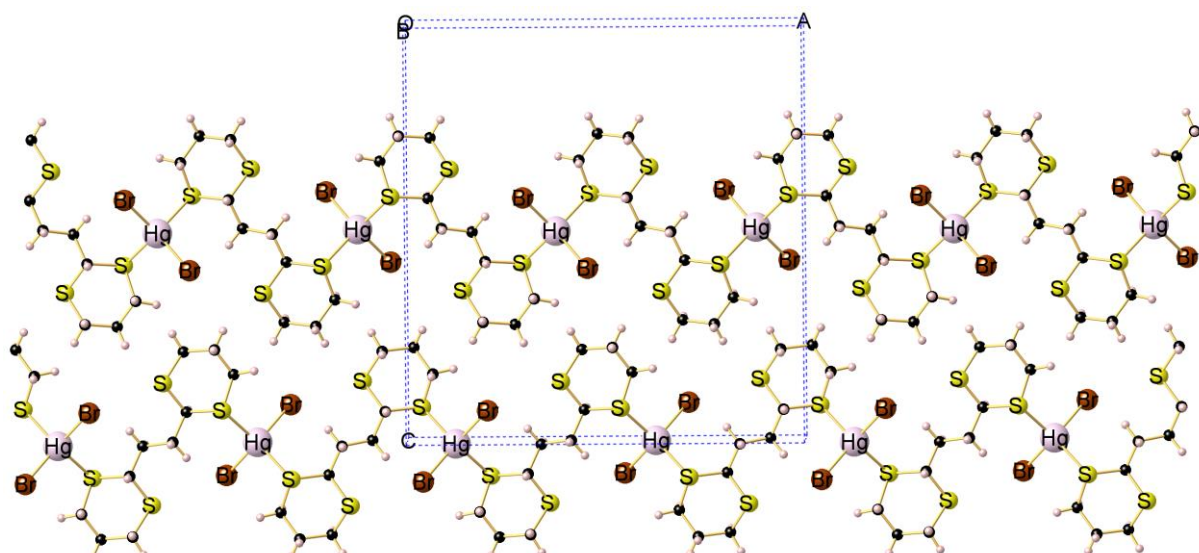


Figure S8. View of the unit cell of CP9 containing two parallel running 1D ribbons.

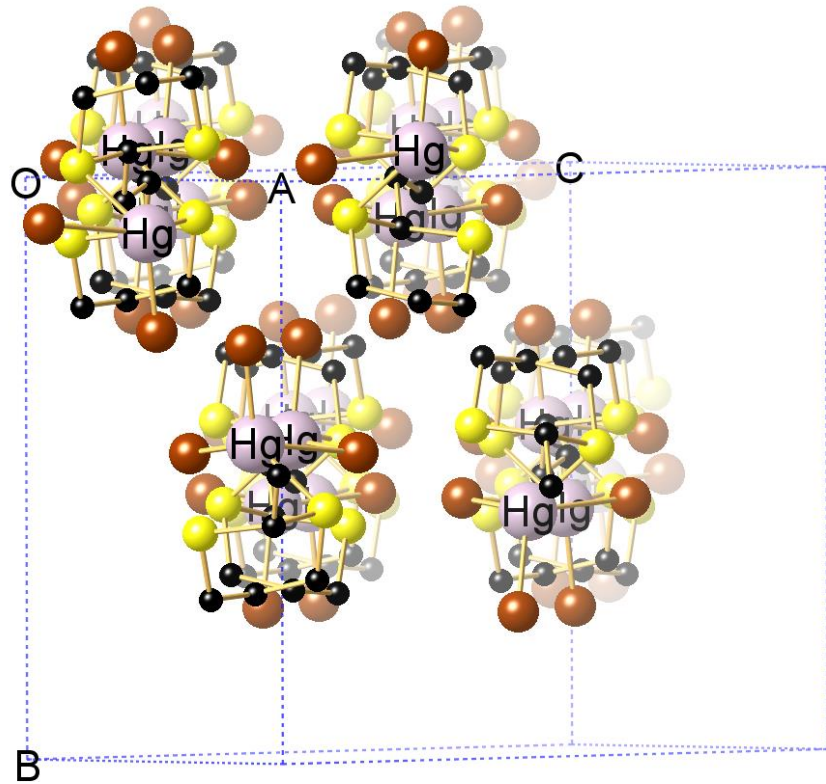


Figure S9. View of the packing of the ribbons of **CP10** within the unit cell.

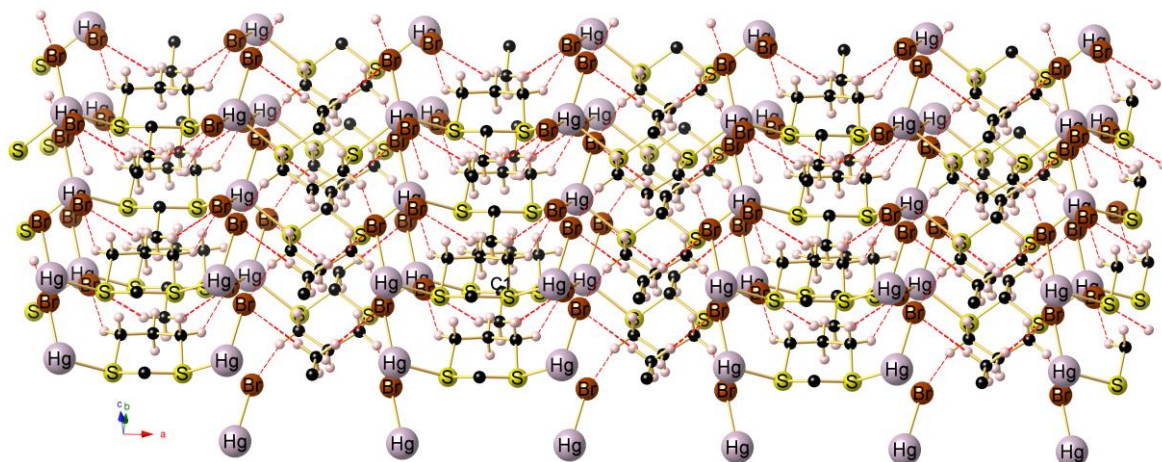


Figure S10. View of the association of parallel running 1D chains of $[(\text{HgBr}_2)(\mu_2\text{-L2})]_n$ (**CP11**) through intermolecular $\text{H}\dots\text{Br}$ bonding generating a 3D supramolecular network.

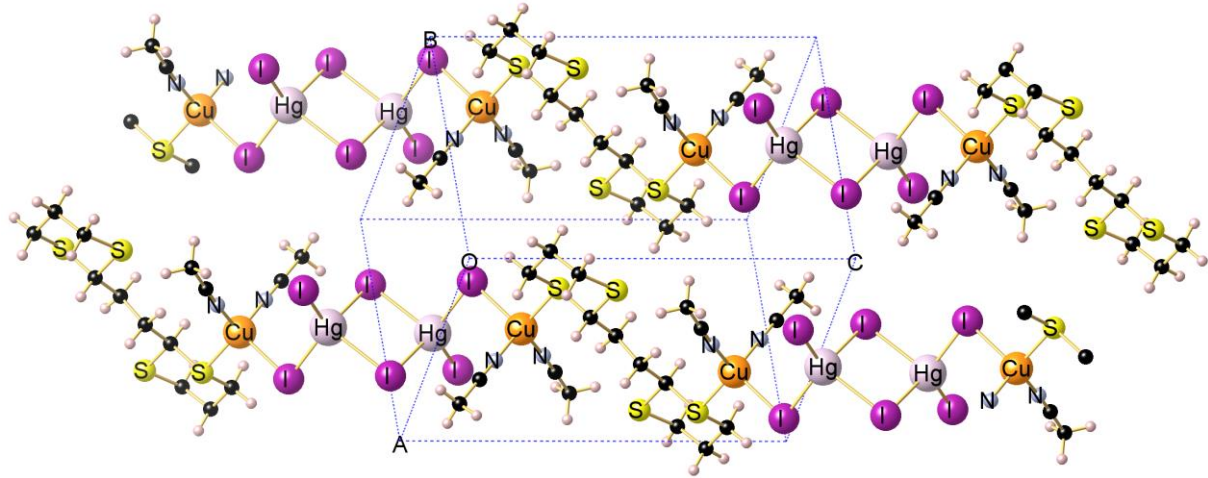


Figure S11. Parallel arrangement of the ribbons of **CP13** in the packing.

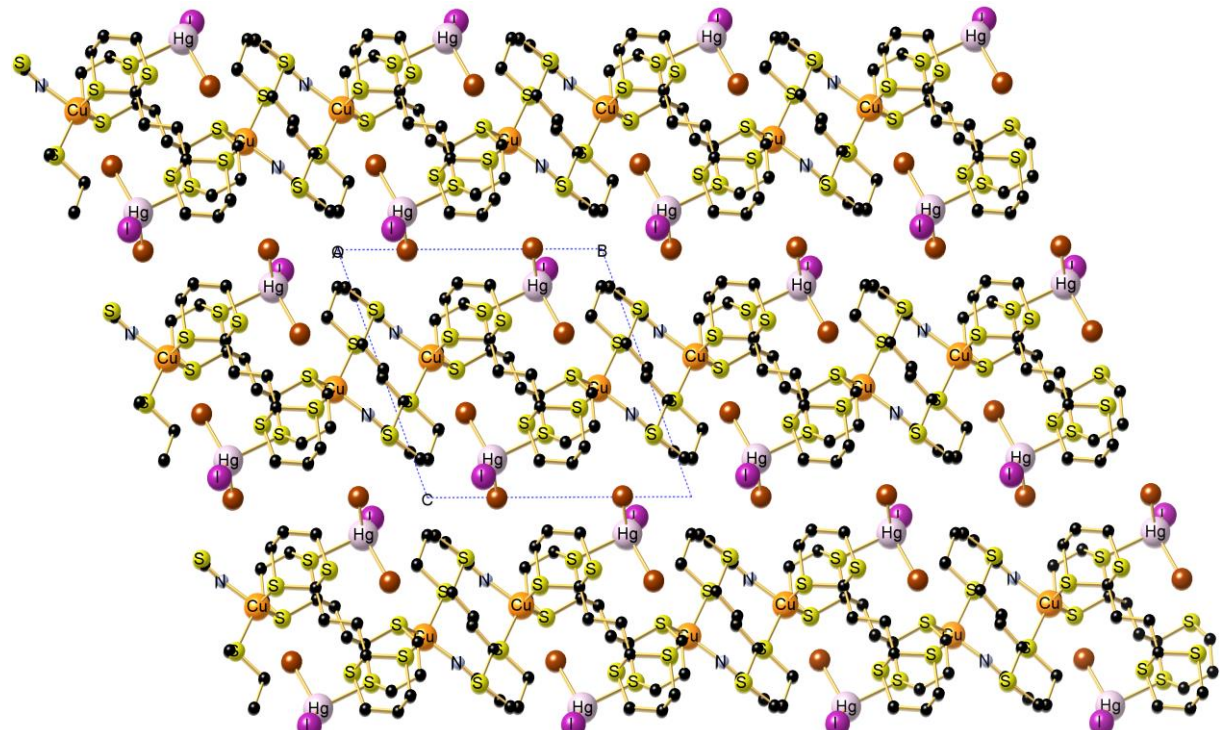


Figure S12. View of the packing of three layers of the 2D network of $\{ \text{Cu}(\text{MeCN}) \} (\text{HgIBr}_2)(\mu_2\text{-L1})_{1.5}]_n$ (**CP15**).

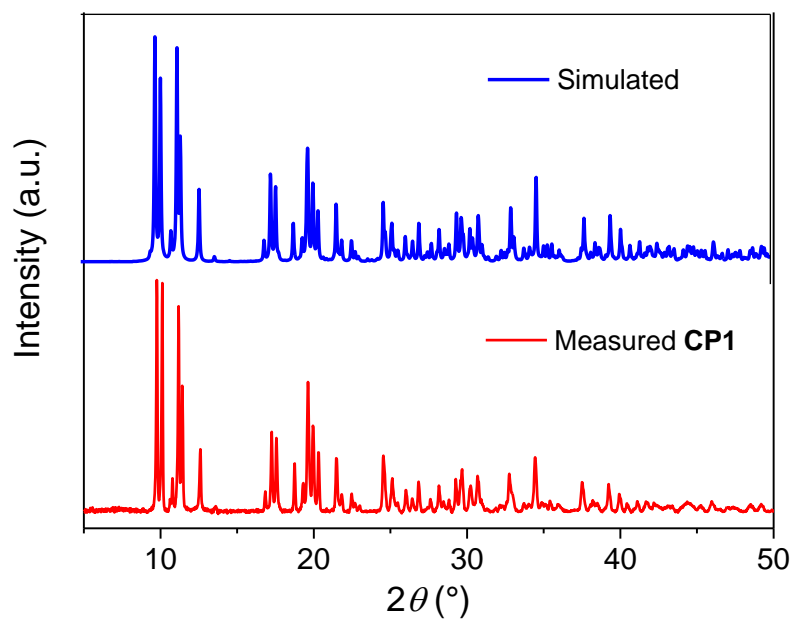


Figure S13. Simulated and experimental PXRD patterns of **CP1**.

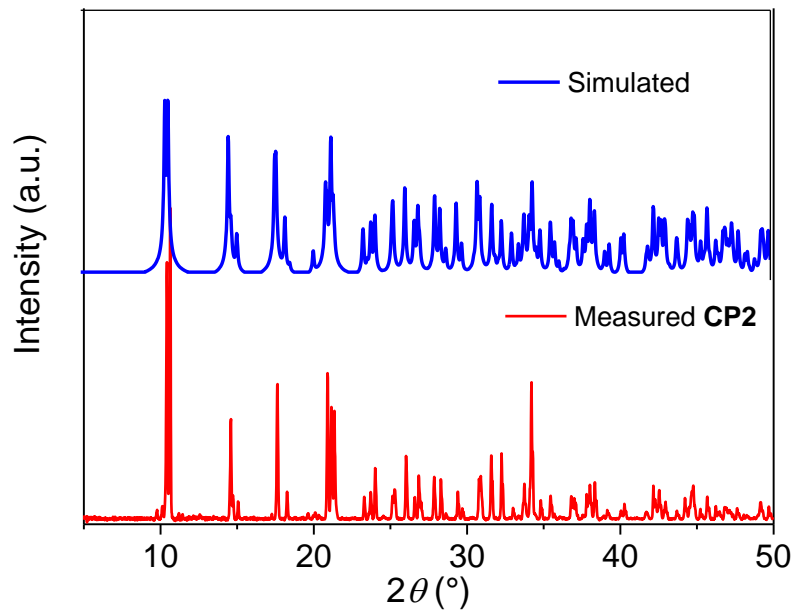


Figure S14. Simulated and experimental PXRD patterns of **CP2**.

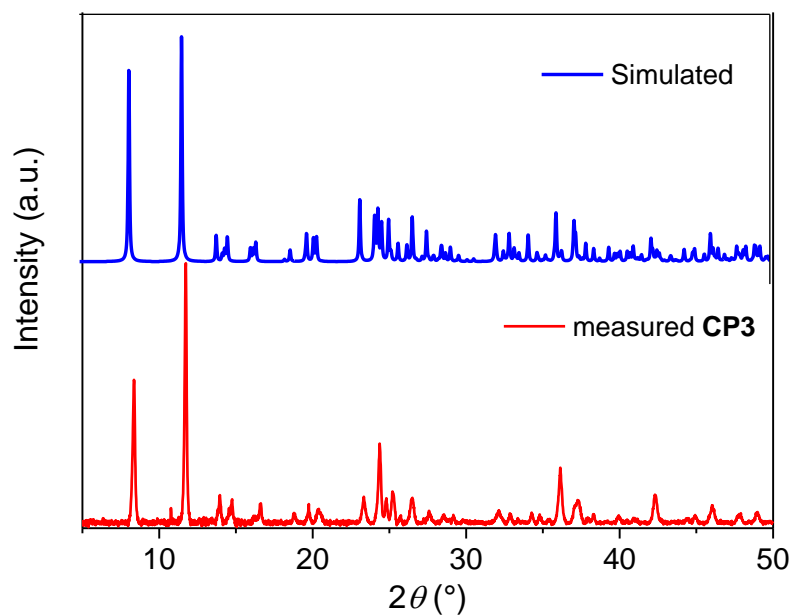


Figure S15. Simulated and experimental PXRD patterns of **CP3**.

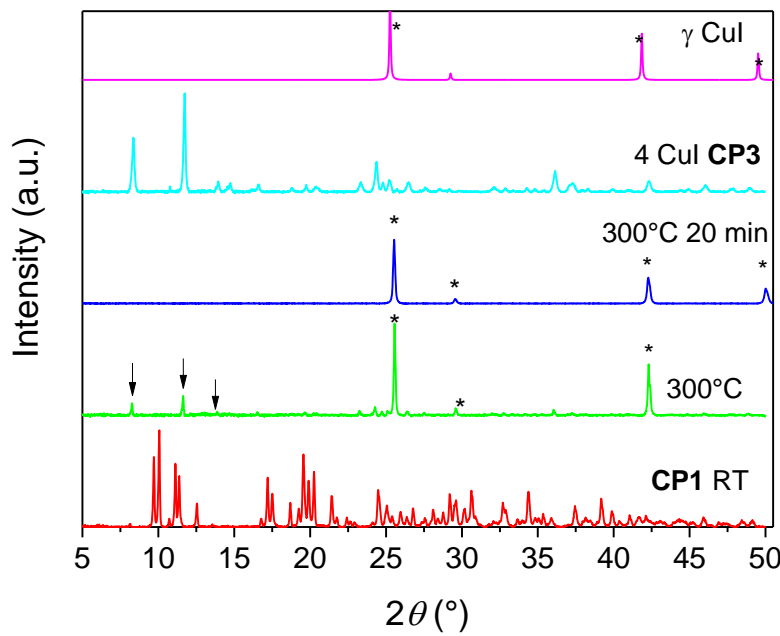


Figure S16. PXRD pattern of **CP1** before and after heating at 300°C. Arrows and asterisk are assigned to **CP3** and γ -CuI respectively.

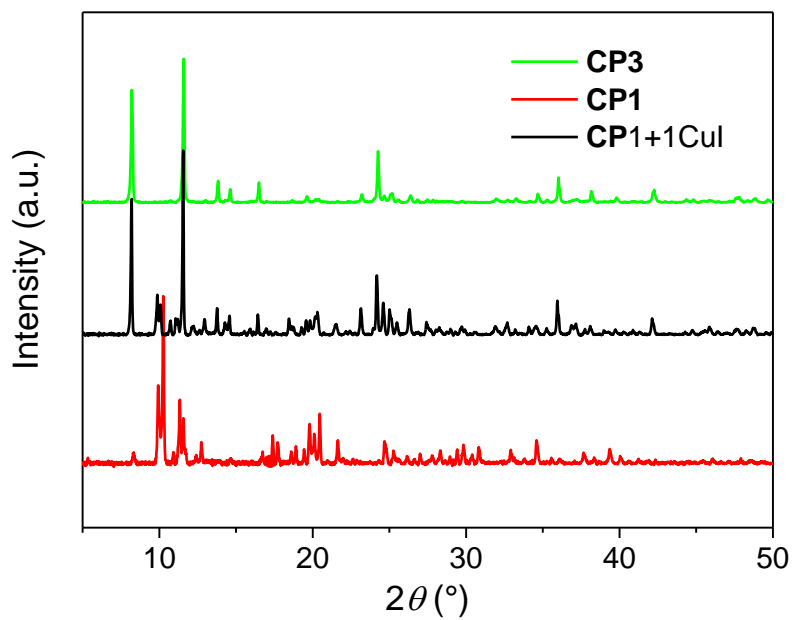


Figure S17. PXRD pattern of **CP1** before and after addition of 1 equivalent CuI. Comparison with the PXRD of **CP3**.

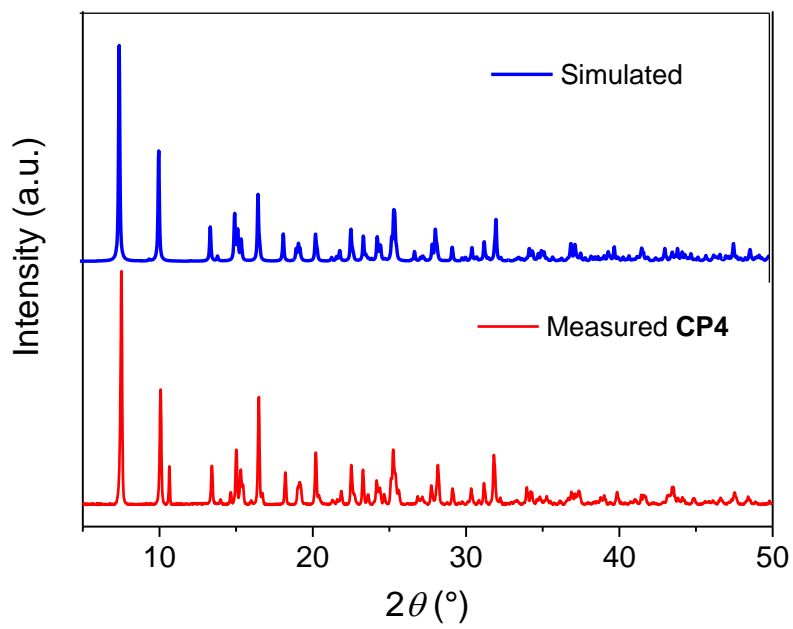


Figure S18. Simulated and experimental PXRD patterns of **CP4**.

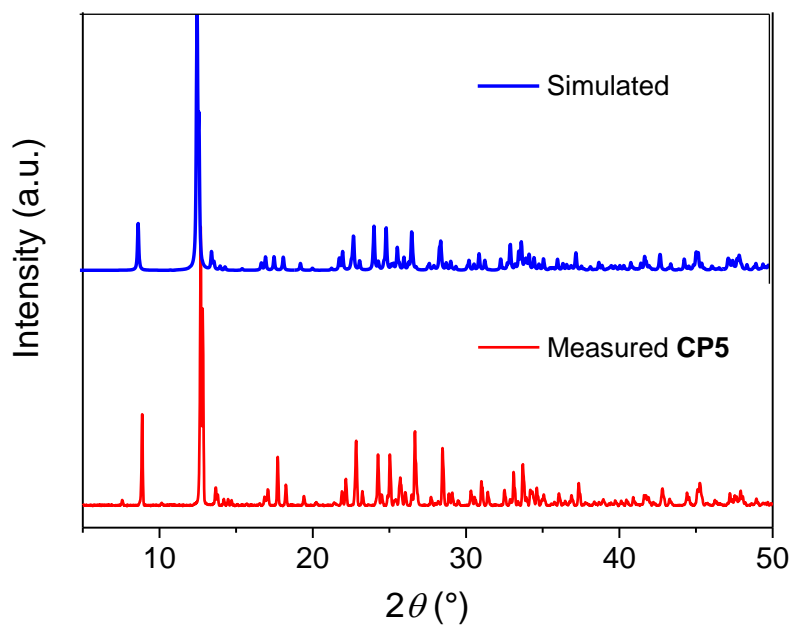


Figure S19. Simulated and experimental PXRD patterns of **CP5**.

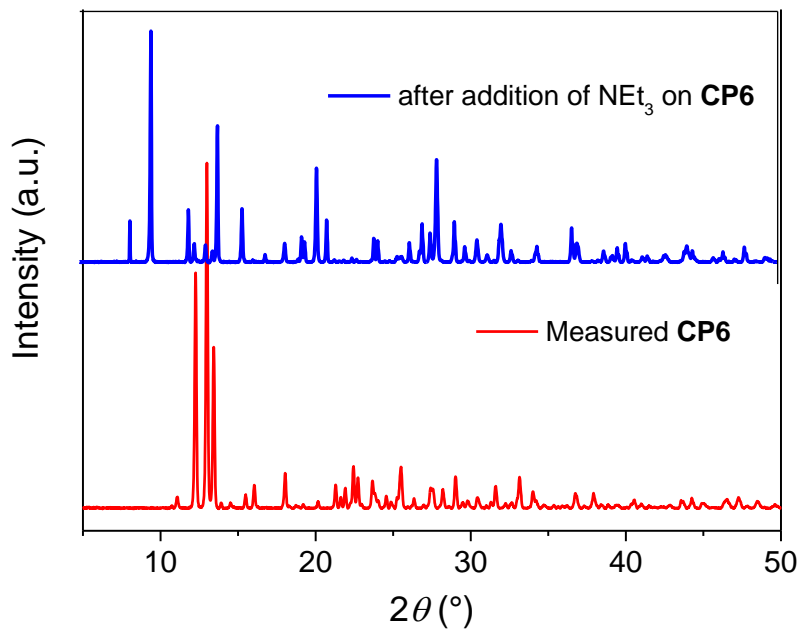


Figure S20. PXRD patterns of **CP6** before and after exposure to NEt_3 .

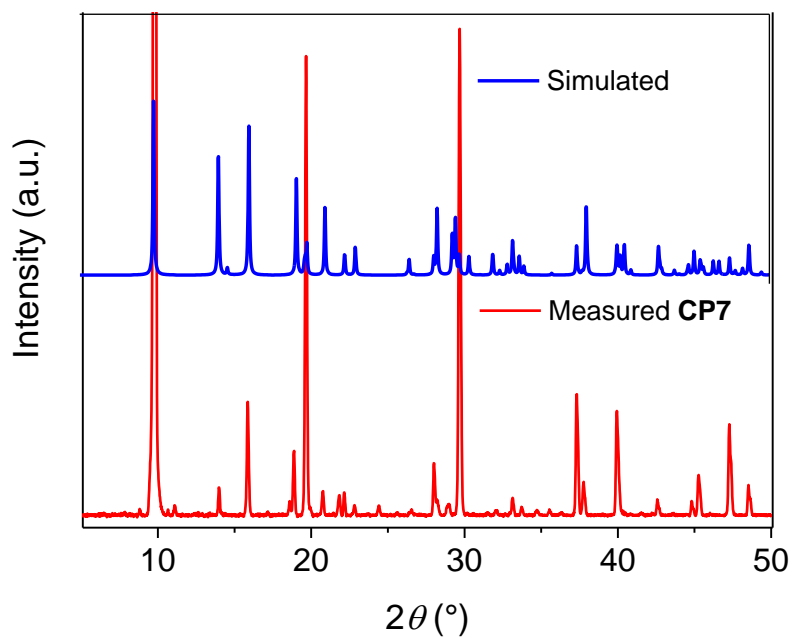


Figure S21. Simulated and experimental PXRD patterns of **CP7**.

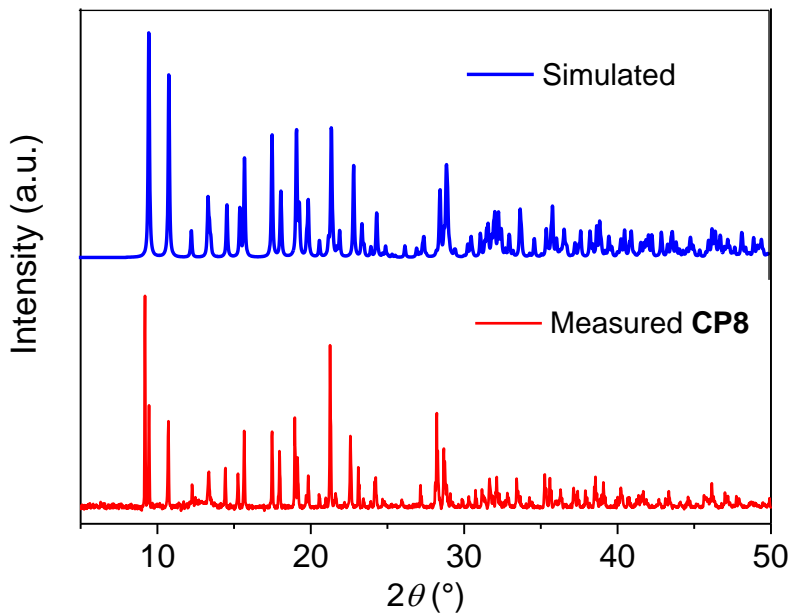


Figure S22. Simulated and experimental PXRD patterns of **CP8**.

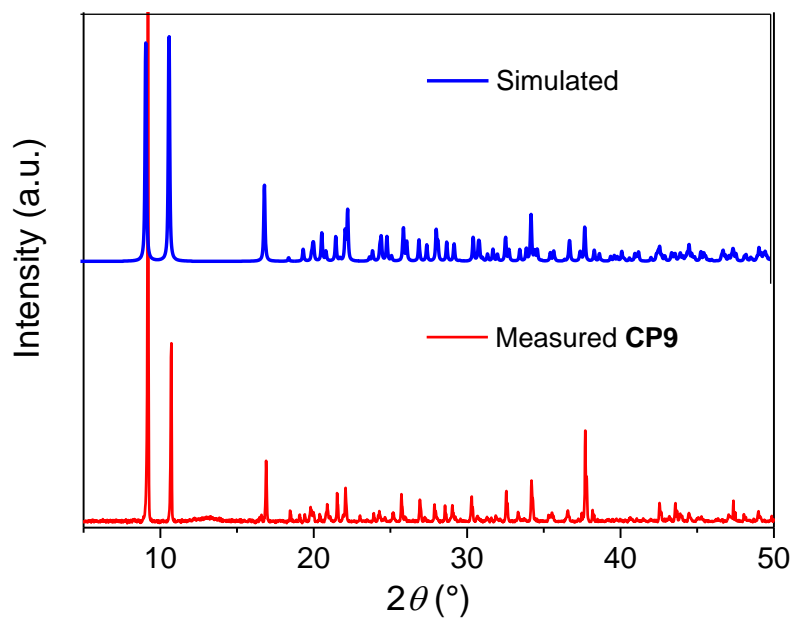


Figure S23. Simulated and experimental PXRD patterns of **CP9**.

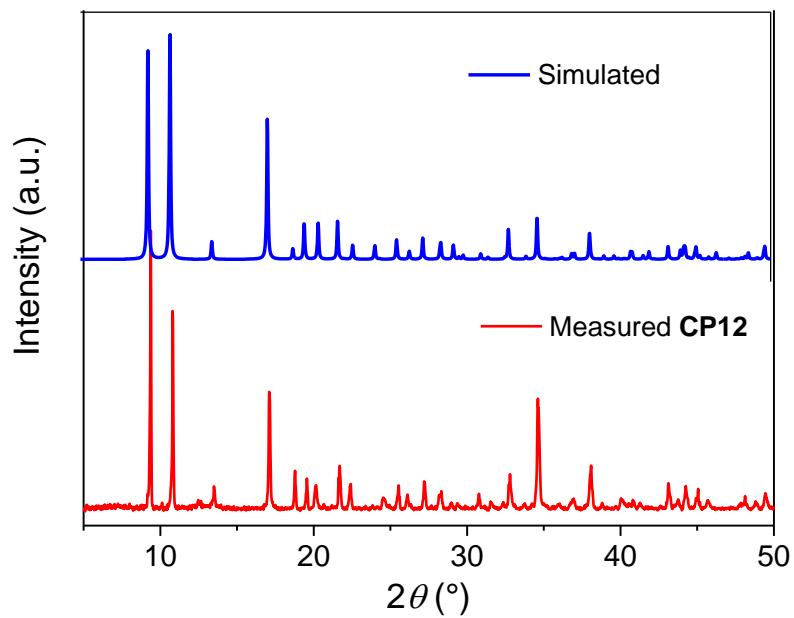


Figure S24. Simulated and experimental PXRD patterns of **CP12**.

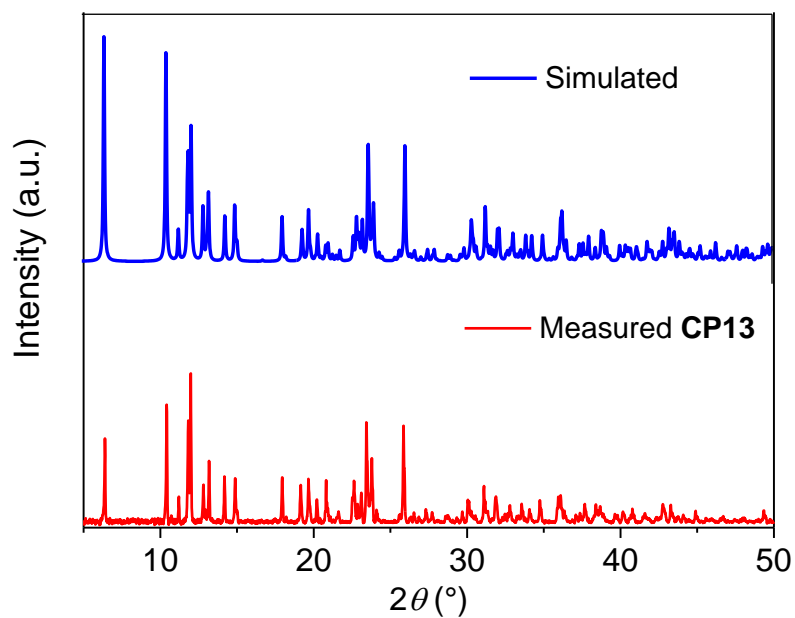


Figure S25. Simulated and experimental PXRD patterns of **CP13**.

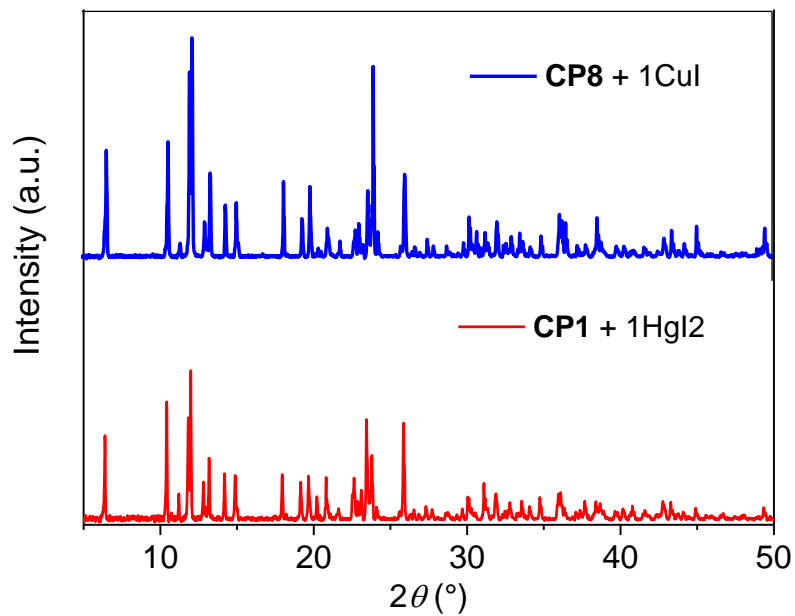


Figure S26. Experimental PXRD patterns of **CP13** obtained by addition of 1CuI to **CP8** and of 1HgI2 to **CP1**.

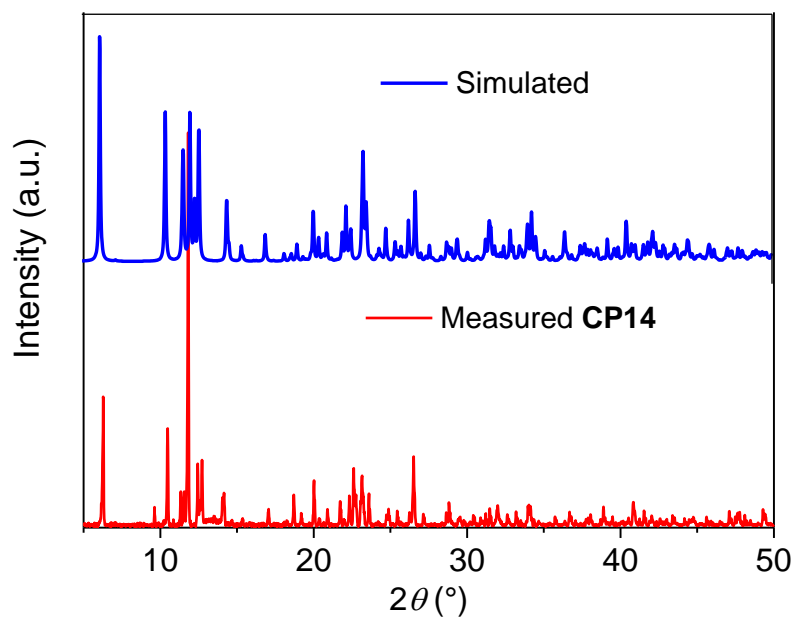


Figure S27. Simulated and experimental PXRD patterns of **CP14**.

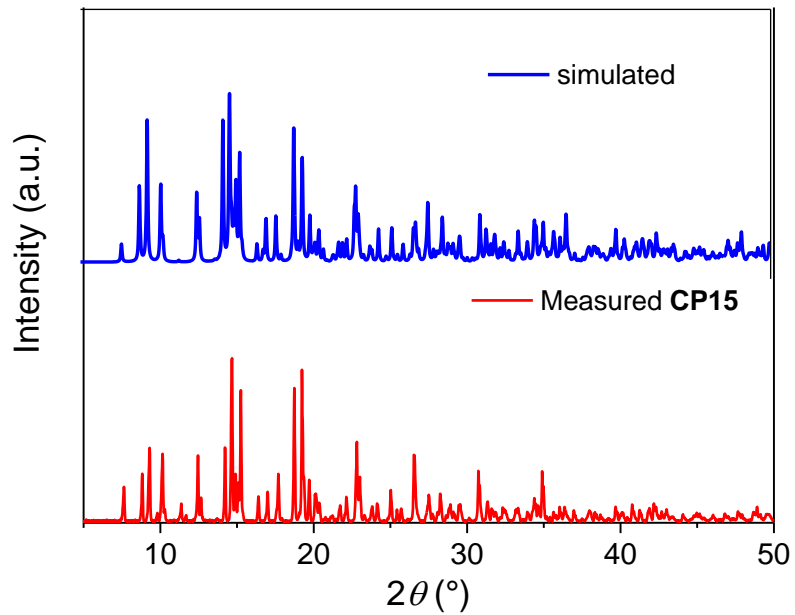


Figure S28. Simulated and experimental PXRD patterns of **CP15**.

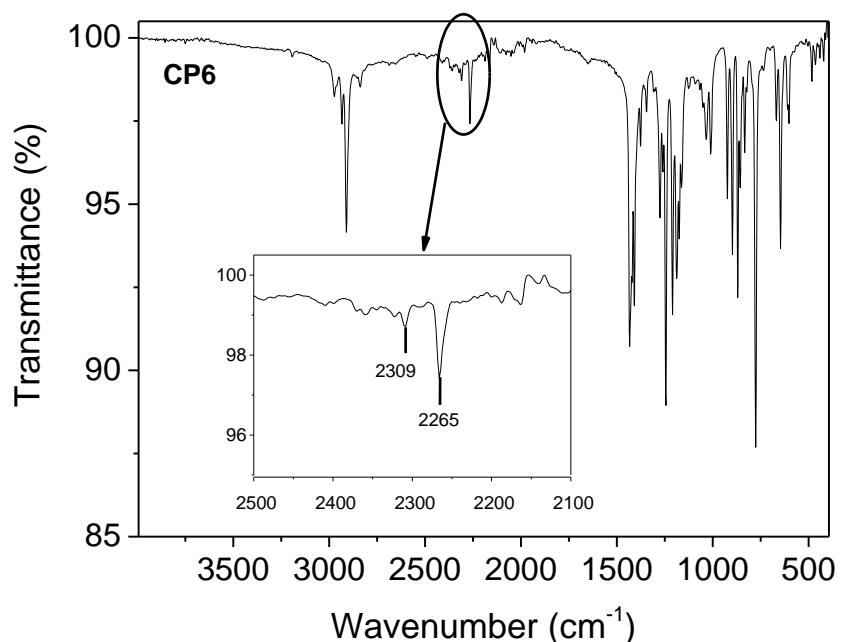


Figure S29. ATR-IR spectrum of **CP6**.

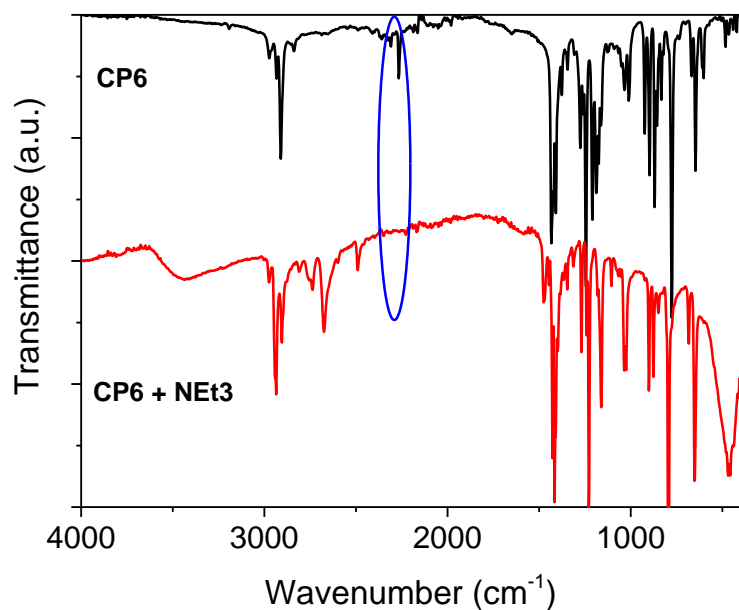


Figure S30. IR spectra of **CP6** before and after exposure to NEt₃.

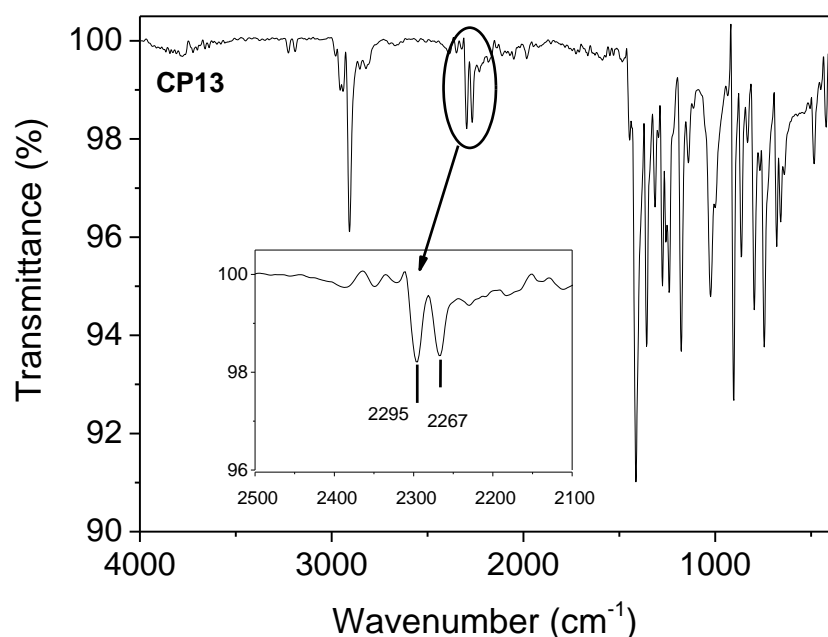


Figure S31. ATR-IR spectrum of **CP13**.

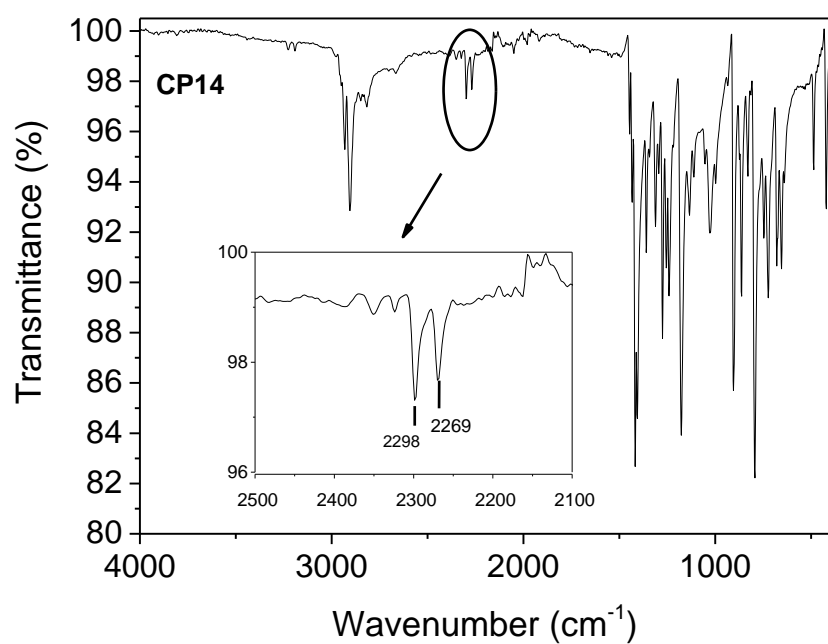


Figure S32. ATR-IR spectrum of **CP14**.

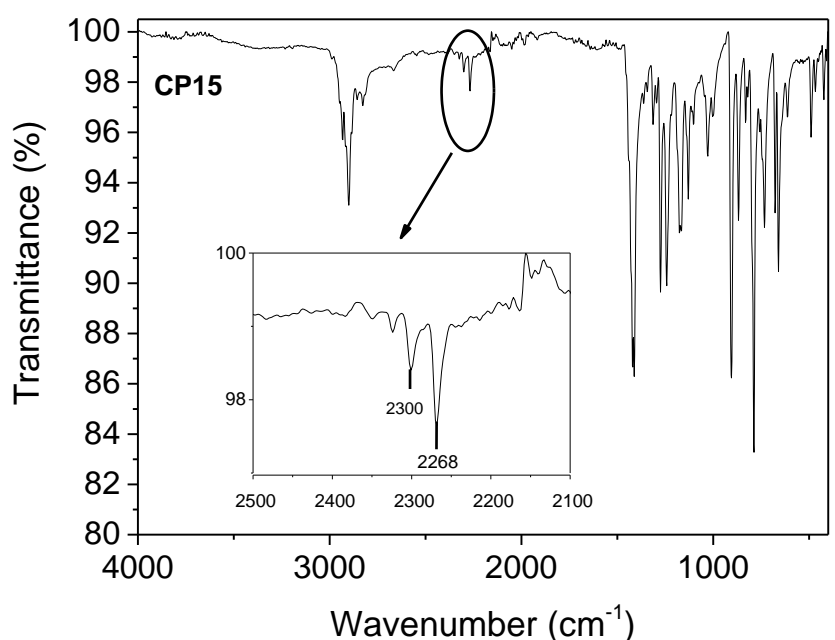


Figure S33. ATR-IR spectrum of **CP15**.

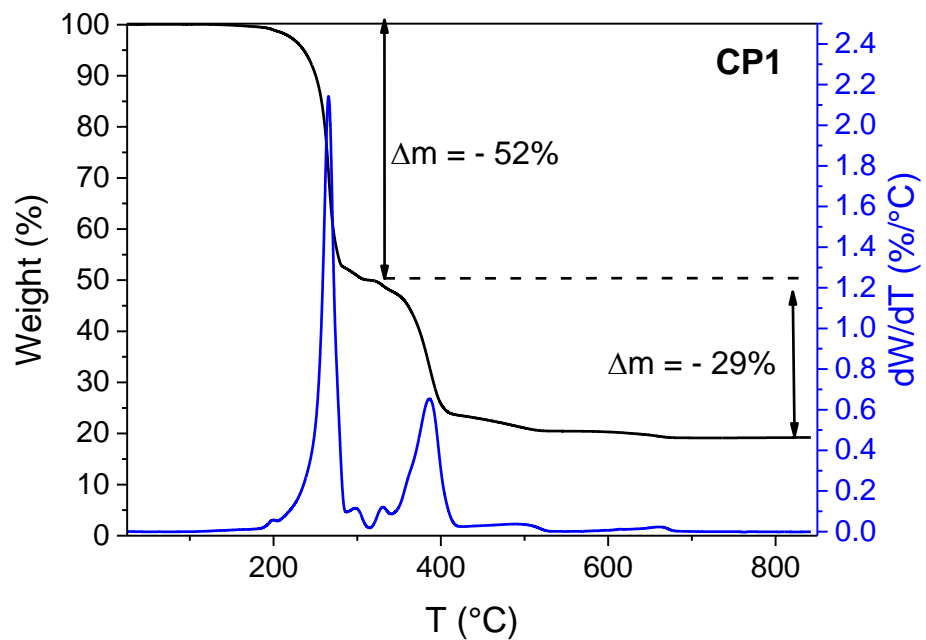


Figure S34. TGA traces and its first derivatives of **CP1** under air flow.

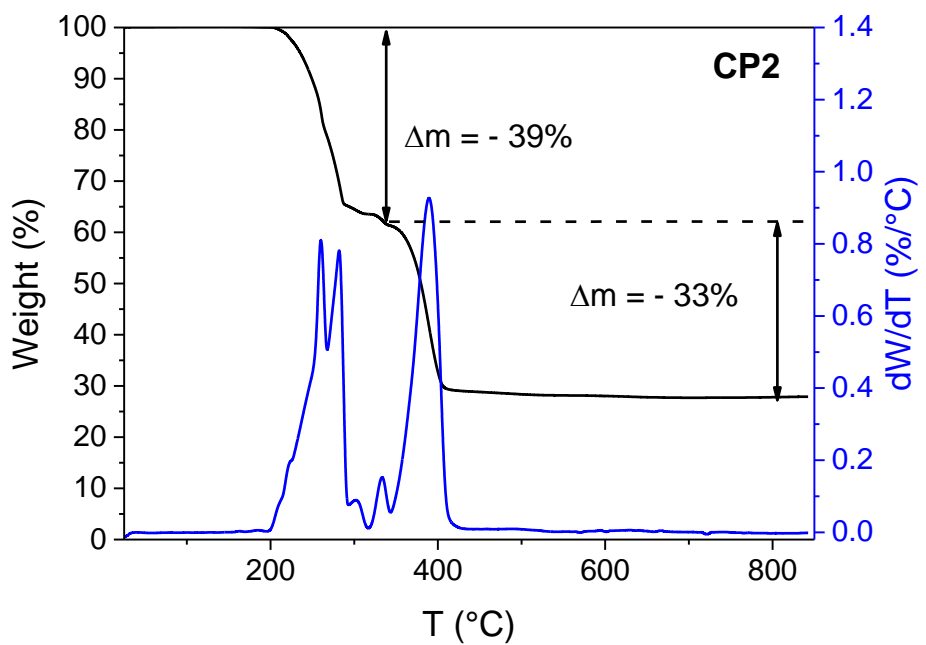


Figure S35. TGA traces and its first derivatives of **CP2** under air flow.

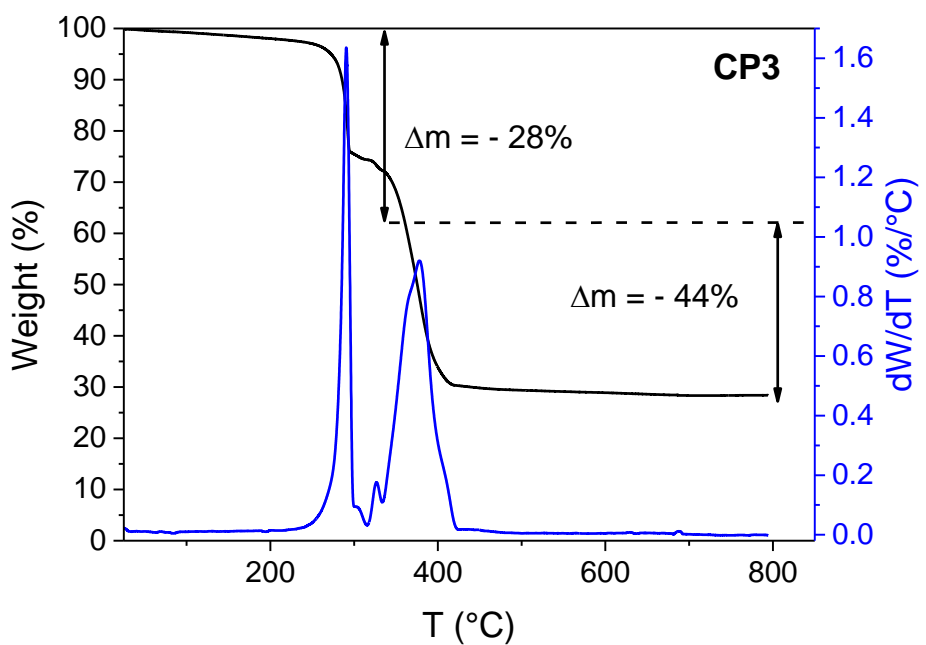


Figure S36. TGA traces and its first derivatives of **CP3** under air flow.

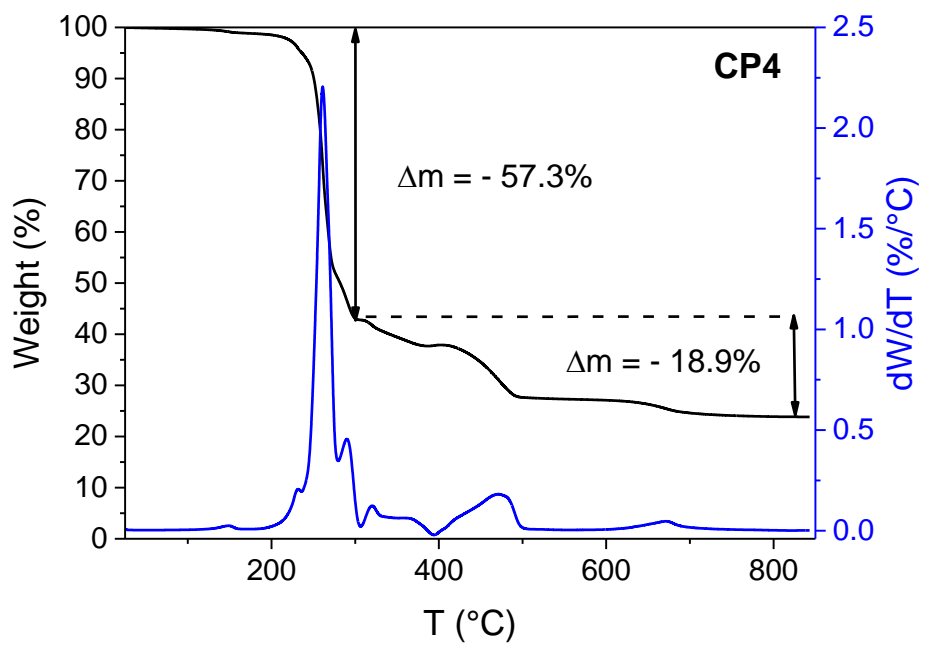


Figure S37. TGA traces and its first derivatives of **CP4** under air flow.

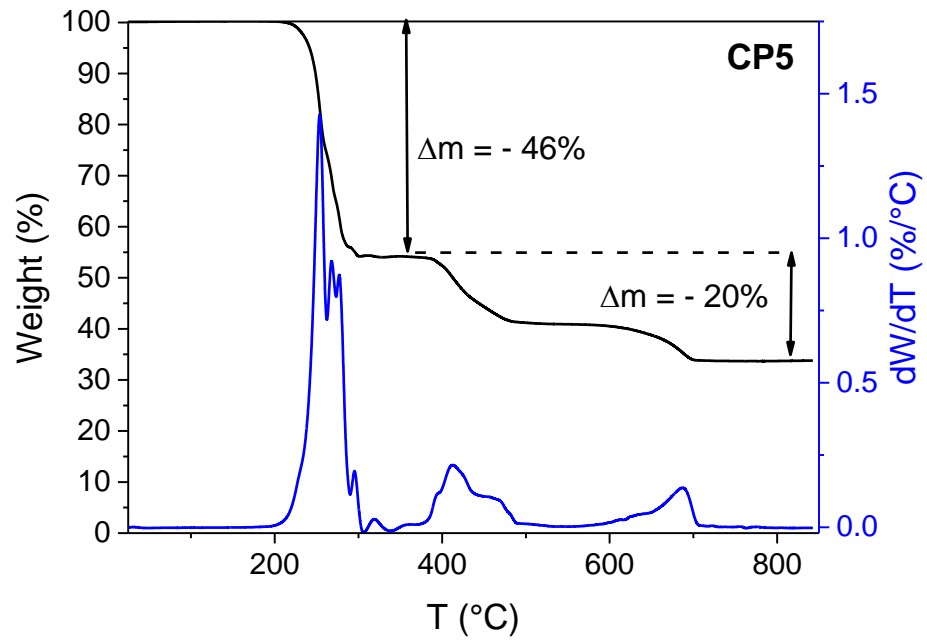


Figure S38. TGA traces and its first derivatives of **CP5** under air flow.

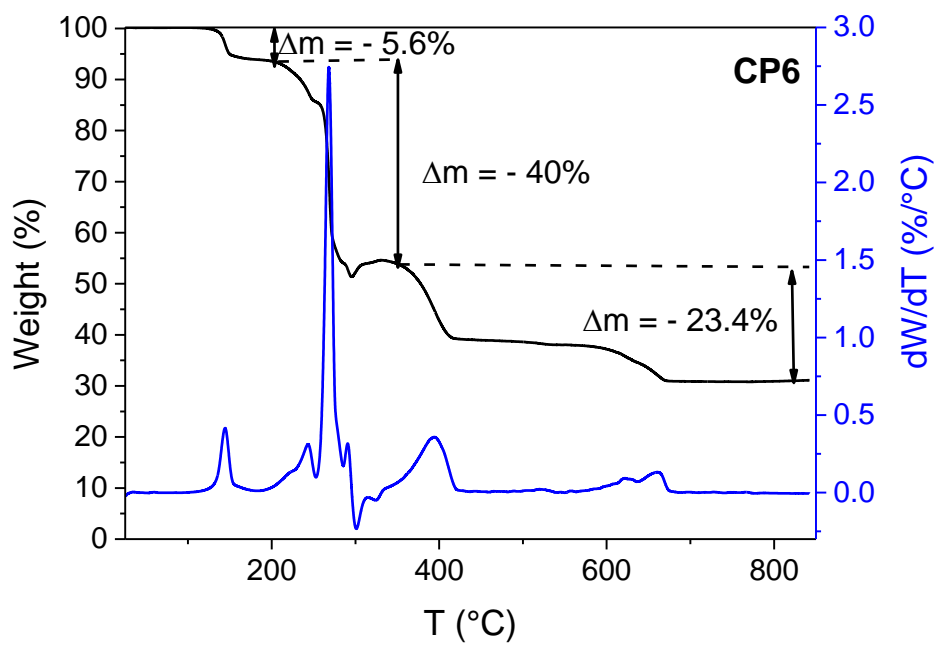


Figure S39. TGA traces and its first derivatives of **CP6** under air flow.

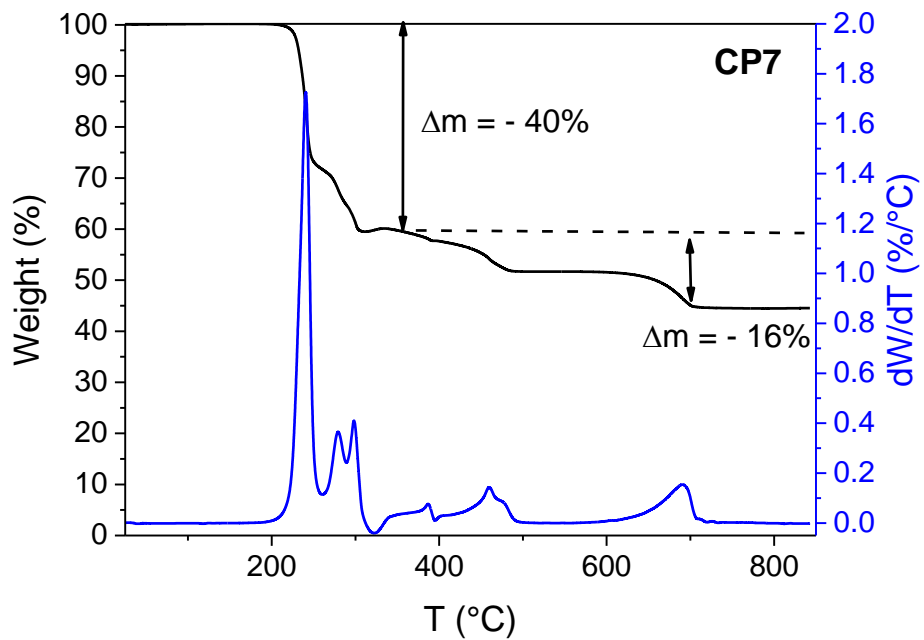


Figure S40. TGA traces and its first derivatives of **CP7** under air flow.



NEt_3

→



Figure S41. Images of **CP6** before and after exposure to NEt_3 vapor.

Table S1. Crystal Data, Data Collection and Structure Refinement for **L1** and **CP1**.

Compound	L1	CP1
Formula	C ₁₀ H ₁₈ S ₄	C ₄₀ H ₇₂ Cu ₄ I ₄ S ₁₆
Formula weight	266.48	1827.69
Temperature/K	100.0	100.0
Wavelength/Å	0.71073	0.71073
Crystal system	monoclinic	monoclinic
Space group	P2 ₁ /n	P2 ₁ /n
<i>a</i> /Å	4.8578(3)	18.4505(6)
<i>b</i> /Å	10.6581(6)	18.2209(5)
<i>c</i> /Å	12.0302(11)	19.1191(7)
$\alpha/^\circ$	90	90
$\beta/^\circ$	92.676(4)	110.0440(10)
$\gamma/^\circ$	90	90
Volume/ Å ³	622.18(8)	6038.2(3)
<i>Z</i>	2	4
Density (calc.) g/cm ³	1.422	2.010
Absorption coefficient/mm ⁻¹	0.725	4.018
<i>F</i> (000)	284.0	3584.0
Crystal size/mm ³	1.177 × 0.158 × 0.14	0.453 × 0.384 × 0.062
2θ range for data collection/°	5.108 to 72.732	4.394 to 59.998
Index ranges	-8 ≤ <i>h</i> ≤ 8, -17 ≤ <i>k</i> ≤ 17, -18 ≤ <i>l</i> ≤ 20 12460	-25 ≤ <i>h</i> ≤ 25, -25 ≤ <i>k</i> ≤ 25, -26 ≤ <i>l</i> ≤ 26 121045
Reflections collected		
Independent reflections	3000 [R _{int} = 0.0306]	17609 [R _{int} = 0.0322]
Refinement method	Full-matrix least-squares on <i>F</i> ²	Full-matrix least-squares on <i>F</i> ²
Data / restraints / parameters	3000/0/64	17609/0/588
Goodness-of-fit on <i>F</i> ²	1.057	1.082
Final <i>R</i> indices [<i>I</i> >2σ(<i>I</i>)]	R ₁ = 0.0215, wR ₂ = 0.0545	R ₁ = 0.0205, wR ₂ = 0.0449
<i>R</i> indices (all data)	R ₁ = 0.0255, wR ₂ = 0.0566	R ₁ = 0.0253, wR ₂ = 0.0478
Largest diff. peak and hole/e. Å ⁻³	0.44/-0.28	2.09/-1.05

Table S2. Crystal Data, Data Collection and Structure Refinement for **CP2** and **CP3**.

Compound	CP2	CP3
Formula	C ₁₀ H ₁₈ Cu ₂ I ₂ S ₄	C ₅ H ₉ Cu ₂ I ₂ S ₂
Formula weight	647.36	514.12
Temperature/K	100.0	100.0
Wavelength/Å	0.71073	0.71073
Crystal system	triclinic	triclinic
Space group	P-1	P-1
<i>a</i> /Å	6.0654(2)	6.6244(19)
<i>b</i> /Å	8.2884(3)	7.837(3)
<i>c</i> /Å	8.4381(3)	11.230(4)
$\alpha/^\circ$	88.411(2)	83.032(11)
$\beta/^\circ$	87.976(2)	73.216(10)
$\gamma/^\circ$	86.729(2)	75.644(12)
Volume/ Å ³	423.11(3)	540.0(3)
<i>Z</i>	1	2
Density (calc.) g/cm ³	2.541	3.162
Absorption coefficient/mm ⁻¹	6.635	9.981
<i>F</i> (000)	306.0	470.0
Crystal size/mm ³	0.114 × 0.062 × 0.059	0.416 × 0.075 × 0.065
2θ range for data collection/°	4.832 to 56.984	3.794 to 52.01
Index ranges	-8 ≤ <i>h</i> ≤ 8, -11 ≤ <i>k</i> ≤ 11, -11 ≤ <i>l</i> ≤ 11 14022	7 ≤ <i>h</i> ≤ 8, -9 ≤ <i>k</i> ≤ 9, -13 ≤ <i>l</i> ≤ 13 2113
Reflections collected	2144 [R _{int} = 0.0465]	2113 [R _{int} = ?,]
Independent reflections	Full-matrix least-squares on <i>F</i> ²	Full-matrix least-squares on <i>F</i> ²
Refinement method	2144/0/82	2113/0/101
Data / restraints / parameters	1.108	1.085
Goodness-of-fit on <i>F</i> ²	R ₁ = 0.0257, wR ₂ = 0.0559	R ₁ = 0.0269, wR ₂ = 0.0753
Final <i>R</i> indices [<i>I</i> >2σ(<i>I</i>)]	R ₁ = 0.0328, wR ₂ = 0.0592	R ₁ = 0.0285, wR ₂ = 0.0767
<i>R</i> indices (all data)	0.96/-0.81	1.88/-0.82
Largest diff. peak and hole/e. Å ⁻³		

Table S3. Crystal Data, Data Collection and Structure Refinement for **CP4** and **CP5**.

Compound	CP4	CP5
Formula	C ₁₅ H ₂₇ Br ₂ Cu ₂ S ₆	C ₁₀ H ₁₈ Br ₂ Cu ₂ S ₄
Formula weight	686.62	553.38
Temperature/K	100.0	100.0
Wavelength/Å	0.71073	0.71073
Crystal system	monoclinic	monoclinic
Space group	P2 ₁ /c	P2 ₁ /c
<i>a</i> /Å	12.9413(15)	8.1301(12)
<i>b</i> /Å	13.0872(11)	13.8417(14)
<i>c</i> /Å	14.5879(17)	14.591(2)
$\alpha/^\circ$	90	90
$\beta/^\circ$	115.754(5)	95.315(7)
$\gamma/^\circ$	90	90
Volume/ Å ³	2225.3(4)	1634.9(4)
<i>Z</i>	4	4
Density (calc.) g/cm ³	2.049	2.248
Absorption coefficient/mm ⁻¹	6.065	7.979
<i>F</i> (000)	1364.0	1080.0
Crystal size/mm ³	0.294 × 0.125 × 0.043	0.133 × 0.084 × 0.034
2θ range for data collection/°	4.392 to 61.136	5.608 to 64.994
Index ranges	18 ≤ <i>h</i> ≤ 18, -18 ≤ <i>k</i> ≤ 15, -20 ≤ <i>l</i> ≤ 20 47344	-12 ≤ <i>h</i> ≤ 12, -20 ≤ <i>k</i> ≤ 20, -22 ≤ <i>l</i> ≤ 22 62361
Reflections collected		
Independent reflections	6754 [R _{int} = 0.0547]	5923 [R _{int} = 0.0370]
Refinement method	Full-matrix least-squares on <i>F</i> ²	Full-matrix least-squares on F ²
Data / restraints / parameters	6754/0/226	5923/0/163
Goodness-of-fit on <i>F</i> ²	1.047	1.088
Final <i>R</i> indices [<i>I</i> >2σ(<i>I</i>)]	R ₁ = 0.0346, wR ₂ = 0.0596	R ₁ = 0.0303, wR ₂ = 0.0721
<i>R</i> indices (all data)	R ₁ = 0.0543, wR ₂ = 0.0665	R ₁ = 0.0351, wR ₂ = 0.0740
Largest diff. peak and hole/e. Å ⁻³	0.81/-0.81	1.57/-1.09

Table S4. Crystal Data, Data Collection and Structure Refinement for **CP6** at 100K and 200K.

Compound	CP6	CP6
Formula	C ₂₄ H ₄₂ Br ₆ Cu ₆ N ₂ S ₈	C ₂₄ H ₄₂ Br ₆ Cu ₆ N ₂ S ₈
Formula weight	1475.77	1475.77
Temperature/K	100.0	200K
Wavelength/Å	0.71073	0.71073
Crystal system	triclinic	triclinic
Space group	P-1	P-1
<i>a</i> /Å	7.8786(4)	7.8928(11)
<i>b</i> /Å	9.8046(5)	9.8456(14)
<i>c</i> /Å	26.8573(15)	26.928(4)
$\alpha/^\circ$	87.562(2)	87.555(2)
$\beta/^\circ$	83.924(2)	84.017(2)
$\gamma/^\circ$	87.249(2)	87.229(2)
Volume/ Å ³	2059.14(19)	2077.2(5)
<i>Z</i>	2	2
Density (calc.) g/cm ³	2.380	2.359
Absorption coefficient/mm ⁻¹	9.293	9.212
<i>F</i> (000)	1424.0	1424.0
Crystal size/mm ³	0.163 × 0.107 × 0.043	0.163 × 0.107 × 0.043
2θ range for data collection/°	4.162 to 72.658	4.144 to 67.504
Index ranges	-13 ≤ <i>h</i> ≤ 13, -16 ≤ <i>k</i> ≤ 16, 0 ≤ <i>l</i> ≤ 44 19959	-12 ≤ <i>h</i> ≤ 12, -15 ≤ <i>k</i> ≤ 15, 0 ≤ <i>l</i> ≤ 42 16608
Reflections collected		
Independent reflections	19959 [R _{int} = 0.0504]	16608 [R _{int} = 0.0501]
Refinement method	Full-matrix least-squares on <i>F</i> ²	Full-matrix least-squares on <i>F</i> ²
Data / restraints / parameters	19959/0/417	16608/0/417
Goodness-of-fit on <i>F</i> ²	1.021	1.000
Final <i>R</i> indices [<i>I</i> >2σ(<i>I</i>)]	R ₁ = 0.0279, wR ₂ = 0.0686	R ₁ = 0.0276, wR ₂ = 0.0683
<i>R</i> indices (all data)	R ₁ = 0.0356, wR ₂ = 0.0714	R ₁ = 0.0369, wR ₂ = 0.0715
Largest diff. peak and hole/e. Å ⁻³	0.83/-1.91	1.36/-1.57

Table S5. Crystal Data, Data Collection and Structure Refinement for **CP7** and **CP8**.

Compound	CP7	CP8
Formula	C ₅ H ₉ ClCuS ₂	C ₁₀ H ₁₈ HgI ₂ S ₄
Formula weight	232.23	720.87
Temperature/K	100.0	100.0
Wavelength/Å	0.71073	0.71073
Crystal system	monoclinic	triclinic
Space group	C2/m	P-1
<i>a</i> /Å	18.3202(9)	9.3903(3)
<i>b</i> /Å	6.7228(3)	9.8817(3)
<i>c</i> /Å	6.1576(3)	10.0545(3)
α /°	90	68.8700(10)
β /°	100.814(2)	79.6750(10)
γ /°	90	86.6570(10)
Volume/ Å ³	744.92(6)	856.14(5)
<i>Z</i>	4	2
Density (calc.) g/cm ³	2.071	2.796
Absorption coefficient/mm ⁻¹	3.751	13.062
<i>F</i> (000)	468.0	656.0
Crystal size/mm ³	0.232 × 0.172 × 0.035	0.459 × 0.254 × 0.174
2θ range for data collection/°	4.528 to 61.046	4.408 to 61.156
Index ranges	-26 ≤ <i>h</i> ≤ 26, -9 ≤ <i>k</i> ≤ 9, -8 ≤ <i>l</i> ≤ 8 12880	-13 ≤ <i>h</i> ≤ 13, -14 ≤ <i>k</i> ≤ 13, -14 ≤ <i>l</i> ≤ 13 14810
Reflections collected	1227 [R _{int} = 0.0375]	5243 [R _{int} = 0.0289]
Independent reflections		
Refinement method	Full-matrix least-squares on <i>F</i> ²	Full-matrix least-squares on <i>F</i> ²
Data / restraints / parameters	1227/0/49	5243/0/155
Goodness-of-fit on <i>F</i> ²	1.426	1.189
Final <i>R</i> indices [<i>I</i> >2σ(<i>I</i>)]	R ₁ = 0.0348, wR ₂ = 0.0858	R ₁ = 0.0242, wR ₂ = 0.0590
<i>R</i> indices (all data)	R ₁ = 0.0387, wR ₂ = 0.0871	R ₁ = 0.0244, wR ₂ = 0.0591
Largest diff. peak and hole/e. Å ⁻³	1.64/-0.70	3.11/-2.46

Table S6. Crystal Data, Data Collection and Structure Refinement for **CP9** and **CP10**.

Compound	CP9	CP10
Formula	C ₁₀ H ₁₈ Br ₂ HgS ₄	C ₅ H ₉ Br ₂ HgS ₂
Formula weight	626.89	493.65
Temperature/K	100.0	100.0
Wavelength/Å	0.71073	0.71073
Crystal system	orthorhombic	monoclinic
Space group	Pna2 ₁	C2/c
<i>a</i> /Å	18.1737(10)	8.2012(3)
<i>b</i> /Å	4.5256(2)	13.2979(5)
<i>c</i> /Å	19.0929(10)	18.6993(7)
$\alpha/^\circ$	90	90
$\beta/^\circ$	90	93.1840(10)
$\gamma/^\circ$	90	90
Volume/ Å ³	1570.33(14)	2036.17(13)
<i>Z</i>	4	8
Density (calc.) g/cm ³	2.652	3.221
Absorption coefficient/mm ⁻¹	15.399	23.309
<i>F</i> (000)	1168.0	1768.0
Crystal size/mm ³	0.217 × 0.105 × 0.034	0.25 × 0.079 × 0.074
2θ range for data collection/°	4.266 to 54.996	5.842 to 61.08
Index ranges	-23 ≤ <i>h</i> ≤ 23, -5 ≤ <i>k</i> ≤ 5, -24 ≤ <i>l</i> ≤ 24	-11 ≤ <i>h</i> ≤ 11, -18 ≤ <i>k</i> ≤ 19, -26 ≤ <i>l</i> ≤ 26
Reflections collected	53635	30365
Independent reflections	3609 [R _{int} = 0.0639]	3110 [R _{int} = 0.0563]
Refinement method	Full-matrix least-squares on <i>F</i> ²	Full-matrix least-squares on <i>F</i> ²
Data / restraints / parameters	3609/1/159	3110/0/91
Goodness-of-fit on <i>F</i> ²	1.066	1.096
Final <i>R</i> indices [<i>I</i> >2σ(<i>I</i>)]	R ₁ = 0.0182, wR ₂ = 0.0441	R ₁ = 0.0214, wR ₂ = 0.0614
<i>R</i> indices (all data)	R ₁ = 0.0204, wR ₂ = 0.0451	R ₁ = 0.0231, wR ₂ = 0.0621
Largest diff. peak and hole/e. Å ⁻³	0.63/-0.53	1.58/-1.94

Table S7. Crystal Data, Data Collection and Structure Refinement for **CP11** and **CP13**.

Compound	CP11	CP13
Formula	C ₁₀ H ₂₀ Br ₄ Hg ₂ S ₄	C ₉ H ₁₅ CuHgI ₃ N ₂ S ₂
Formula weight	989.32	860.18
Temperature/K	100.0	100.00
Wavelength/Å	0.71073	0.71073
Crystal system	orthorhombic	triclinic
Space group	Ama2	P-1
<i>a</i> /Å	14.1565(12)	8.3763(8)
<i>b</i> /Å	15.7413(13)	9.3131(8)
<i>c</i> /Å	4.5260(3)	14.2531(9)
$\alpha/^\circ$	90	94.414(4)
$\beta/^\circ$	90	102.209(4)
$\gamma/^\circ$	90	113.075(4)
Volume/ Å ³	1008.58(14)	983.86(14)
<i>Z</i>	2	2
Density (calc.) g/cm ³	3.258	2.904
Absorption coefficient/mm ⁻¹	23.529	13.780
<i>F</i> (000)	888.0	766.0
Crystal size/mm ³	0.128 × 0.122 × 0.046	0.287 × 0.098 × 0.096
2θ range for data collection/°	5.756 to 66.326	5.202 to 64.998
Index ranges	-21 ≤ <i>h</i> ≤ 21, -24 ≤ <i>k</i> ≤ 24, -6 ≤ <i>l</i> ≤ 6	-12 ≤ <i>h</i> ≤ 12, -14 ≤ <i>k</i> ≤ 14, -21 ≤ <i>l</i> ≤ 21
Reflections collected	8550	185883
Independent reflections	1968 [R _{int} = 0.0341]	7116 [R _{int} = 0.0381]
Refinement method	Full-matrix least-squares on <i>F</i> ²	Full-matrix least-squares on <i>F</i> ²
Data / restraints / parameters	1968/1/51	7116/0/165
Goodness-of-fit on <i>F</i> ²	0.969	1.116
Final <i>R</i> indices [<i>I</i> >2σ(<i>I</i>)]	R ₁ = 0.0176, wR ₂ = 0.0385	R ₁ = 0.0204, wR ₂ = 0.0543
<i>R</i> indices (all data)	R ₁ = 0.0196, wR ₂ = 0.0397	R ₁ = 0.0212, wR ₂ = 0.0556
Largest diff. peak and hole/e. Å ⁻³	1.00/-0.97	2.80/-2.03

Table S8. Crystal Data, Data Collection and Structure Refinement for **CP14** and **CP15**.

Compound	CP14	CP15
Formula	$C_{22}H_{38}Cu_2Hg_2I_6N_4S_4$	$C_{17}H_{30}Br_2CuHgINS_6$
Formula weight	1776.46	991.86
Temperature/K	100.0	100.00
Wavelength/Å	0.71073	0.71073
Crystal system	triclinic	triclinic
Space group	P-1	P-1
<i>a</i> /Å	9.8483(8)	10.1654(12)
<i>b</i> /Å	14.9259(16)	12.582(2)
<i>c</i> /Å	15.2501(13)	13.033(2)
$\alpha/^\circ$	108.914(3)	67.070(7)
$\beta/^\circ$	95.043(5)	69.373(5)
$\gamma/^\circ$	94.515(3)	76.469(6)
Volume/ Å ³	2098.7(3)	1427.8(4)
<i>Z</i>	2	2
Density (calc.) g/cm ³	2.811	2.307
Absorption coefficient/mm ⁻¹	12.924	10.439
<i>F</i> (000)	1596.0	934.0
Crystal size/mm ³	0.199 × 0.169 × 0.142	0.199 × 0.072 × 0.041
2θ range for data collection/°	4.694 to 64,998	4.716 to 61.124
Index ranges	-14 ≤ <i>h</i> ≤ 14, -22 ≤ <i>k</i> ≤ 22, -23 ≤ <i>l</i> ≤ 23	-13 ≤ <i>h</i> ≤ 14, -17 ≤ <i>k</i> ≤ 17, -18 ≤ <i>l</i> ≤ 18
Reflections collected	732333	38896
Independent reflections	15174 [R _{int} = 0.0705]	8594 [R _{int} = 0.0318]
Refinement method	Full-matrix least-squares on <i>F</i> ²	Full-matrix least-squares on <i>F</i> ²
Data / restraints / parameters	15174/0/452	8594/0/284
Goodness-of-fit on <i>F</i> ²	1.115	1.098
Final <i>R</i> indices [<i>I</i> >2σ(<i>I</i>)]	R ₁ = 0.0153, wR ₂ = 0.0366	R ₁ = 0.0229, wR ₂ = 0.0354
<i>R</i> indices (all data)	R ₁ = 0.0160, wR ₂ = 0.0370	R ₁ = 0.0316, wR ₂ = 0.0377
Largest diff. peak and hole/e. Å ⁻³	1.20/-1.43	0.80/-0.93

Table S9. Crystal Data, Data Collection and Structure Refinement for **D1** and **M1**.

Compound	D1	M1
Formula	C ₁₀ H ₂₀ Hg ₂ I ₄ S ₂	C ₁₀ H ₂₀ Br ₂ HgS ₄
Formula weight	1177.28	628.91
Temperature/K	100.0	100.0
Wavelength/Å	0.71073	0.71073
Crystal system	monoclinic	orthorhombic
Space group	P2 ₁ /n	P2 ₁ 2 ₁ 2
<i>a</i> /Å	9.7802(8)	8.2203(3)
<i>b</i> /Å	10.0351(10)	22.7657(9)
<i>c</i> /Å	11.6340(10)	4.4494(2)
α /°	90	90
β /°	90.652(3)	90
γ /°	90	90
Volume/ Å ³	1141.75(18)	832.66(6)
<i>Z</i>	2	2
Density (calc.) g/cm ³	3.424	2.508
Absorption coefficient/mm ⁻¹	19.194	14.521
<i>F</i> (000)	1032.0	588.0
Crystal size/mm ³	0.308 × 0.157 × 0.134	0.332 × 0.044 × 0.037
2θ range for data collection/°	5.472 to 58	6.114 to 55.962
Index ranges	-13 ≤ <i>h</i> ≤ 13, -13 ≤ <i>k</i> ≤ 13, -15 ≤ <i>l</i> ≤ 15	-10 ≤ <i>h</i> ≤ 10, -30 ≤ <i>k</i> ≤ 30, -5 ≤ <i>l</i> ≤ 5
Reflections collected	50811	18946
Independent reflections	3029 [R _{int} = 0.0528]	2004 [R _{int} = 0.0500]
Refinement method	Full-matrix least-squares on <i>F</i> ²	Full-matrix least-squares on <i>F</i> ²
Data / restraints / parameters	3029/0/93	2004/0/85
Goodness-of-fit on <i>F</i> ²	1.187	1.139
Final <i>R</i> indices [<i>I</i> >2σ(<i>I</i>)]	R ₁ = 0.0202, wR ₂ = 0.0462	R ₁ = 0.0192, wR ₂ = 0.0326
<i>R</i> indices (all data)	R ₁ = 0.0203, wR ₂ = 0.0463	R ₁ = 0.0213, wR ₂ = 0.0334
Largest diff. peak and hole/e. Å ⁻³	1.73/-2.73	0.76/-0.92

Table S10. Hydrogen bond geometry (\AA , $^\circ$) in **CP6**.

$D-\text{H}\cdots A$	$D-\text{H}$	$\text{H}\cdots A$	$D\cdots A$	$D-\text{H}\cdots A$
C3—H3A…S7 ¹	0.99	3.05	3.698(4)	124.2
C7—H7…Br3 ²	1.00	2.70	3.649(4)	157.8
C8—H8B…Br2 ²	0.99	2.86	3.598(4)	132.4
C9—H9A…Br2 ³	0.99	3.05	3.695(4)	124.2
C17—H17…Br6 ⁴	1.00	2.72	3.678(4)	161.2
C18—H18A…N1 ⁵	0.99	2.85	3.679(6)	141.2
C20—H20B…Br1 ⁶	0.99	2.95	3.679(4)	131.3
C22—H22B…Br1 ⁴	0.98	2.85	3.692(5)	144.2
C22—H22C…Br5 ⁶	0.98	2.94	3.621(5)	127.2

Symmetry codes: ¹1+X,-1+Y,+Z; ²1+X,+Y,+Z; ³1-X,-Y,1-Z; ⁴-1+X,+Y,+Z; ⁵+X,1+Y,+Z; ⁶1-X,1-Y,2-Z**Table S11.** Hydrogen bond geometry (\AA , $^\circ$) in **CP11**.

$D-\text{H}\cdots A$	$D-\text{H}$	$\text{H}\cdots A$	$D\cdots A$	$D-\text{H}\cdots A$
C1—H1B…Br1 ¹	0.99	3.10	3.758(4)	124.7
C1—H1B…Br1 ²	0.99	2.87	3.667(4)	138.3